cmgh
CELLULAR AND MOLECULAR GASTROENTEROLOGY AND HEPATOLOGY

ORIGINAL RESEARCH

RIPK1 Mediates TNF-Induced Intestinal Crypt Apoptosis During Chronic NF-κB Activation

Jerry Wong,[1,2,3,a] Ricard Garcia-Carbonell,[1,2,3,4,a] Matija Zelic,[5] Samuel B. Ho,[6,7] Brigid S. Boland,[6,8] Shih-Jing Yao,[1,2,3] Shalin A. Desai,[1,2,3] Soumita Das,[3] Núria Planell,[9] Philip A. Harris,[10] Joan Font-Burgada,[1,2,3] Koji Taniguchi,[1,2,3] John Bertin,[5] Azucena Salas,[9] Manolis Pasparakis,[11] Pete J. Gough,[10] Michelle Kelliher,[5] Michael Karin,[1,2,3] and Monica Guma[12,13]

[1]*Laboratory of Gene Regulation and Signal Transduction,* [2]*Department of Pharmacology,* [3]*Department Pathology,* [6]*Division of Gastroenterology, and* [12]*Department Rheumatology,* [8]*San Diego Digestive Disease Research Center, San Diego, California;* [4]*Department of Biochemistry and Molecular Biology, Faculty of Pharmacy, University of Barcelona, Barcelona, Spain,* [5]*Department of Molecular, Cell and Cancer Biology, University of Massachusetts Medical School, Worcester, Massachusetts;* [10]*Pattern Recognition Receptor Discovery Performance Unit, Immuno-Inflammation Therapeutic Area, GlaxoSmithKline, Collegeville, Pennsylvania;* [7]*Department of Medicine, VA San Diego Healthcare System, San Diego, California;* [9]*Department of Gastroenterology, IDIBAPS, Hospital Clínic, CIBER-EHD, Barcelona, Spain;* [11]*Institute for Genetics, Centre for Molecular Medicine and Cologne Excellence Cluster on Cellular Stress Responses in Aging-Associated Diseases, University of Cologne, Cologne, Germany;* [13]*Department of Medicine, Autonomous University of Barcelona, Plaça Cívica, Bellaterra, Barcelona, Spain*

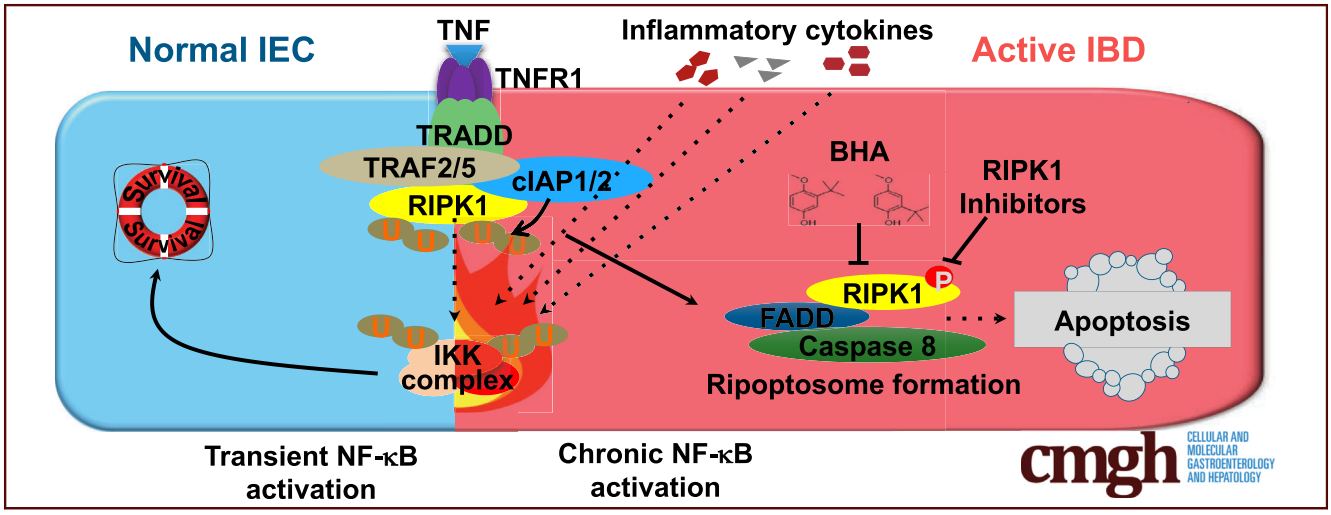

SUMMARY

Here we describe how chronic nuclear factor–κB activation facilitates the formation of the ripoptosome, which enhances tumor necrosis factor–induced apoptosis in intestinal epithelial cells. Blockade of the kinase activity of RIPK1 prevents tumor necrosis factor's destructive properties while preserving its survival and proliferative functions.

BACKGROUND AND AIMS: Tumor necrosis factor (TNF) is a major pathogenic effector and a therapeutic target in inflammatory bowel disease (IBD), yet the basis for TNF-induced intestinal epithelial cell (IEC) death is unknown, because TNF does not kill normal IECs. Here, we investigated how chronic nuclear factor (NF)- κB activation, which occurs in human IBD, promotes TNF-dependent IEC death in mice.

METHODS: Human IBD specimens were stained for p65 and cleaved caspase-3. C57BL/6 mice with constitutively active IKKβ in IEC ($Ikk\beta(EE)^{IEC}$), $Ripk1^{D138N/D138N}$ knockin mice, and $Ripk3^{-/-}$ mice were injected with TNF or lipopolysaccharide. Enteroids were also isolated from these mice and challenged with TNF with or without RIPK1 and RIPK3 inhibitors or butylated hydroxyanisole. Ripoptosome-mediated caspase-8 activation was assessed by immunoprecipitation.

RESULTS: NF-κB activation in human IBD correlated with appearance of cleaved caspase-3. Congruently, unlike normal mouse IECs that are TNF-resistant, IECs in $Ikk\beta(EE)^{IEC}$ mice and enteroids were susceptible to TNF-dependent apoptosis, which depended on the protein kinase function of RIPK1. Constitutively active IKKβ facilitated ripoptosome formation, a RIPK1 signaling complex that mediates caspase-8 activation by TNF. Butylated hydroxyanisole treatment and RIPK1 inhibitors attenuated TNF-induced and ripoptosome-

mediated caspase-8 activation and IEC death *in vitro* and *in vivo*.

CONCLUSIONS: Contrary to common expectations, chronic NF-κB activation induced intestinal crypt apoptosis after TNF stimulation, resulting in severe mucosal erosion. RIPK1 kinase inhibitors selectively inhibited TNF destructive properties while preserving its survival and proliferative properties, which do not require RIPK1 kinase activity. RIPK1 kinase inhibition could be a potential treatment for IBD. *(Cell Mol Gastroenterol Hepatol 2020;9:295–312; https://doi.org/10.1016/j.jcmgh.2019.10.002)*

Keywords: IBD; RIPK1; Intestinal Epithelial Cell; Ripoptosome; Cell Death.

Inflammatory bowel disease (IBD), including ulcerative colitis (UC) and Crohn's disease (CD), represent a major cause of morbidity and mortality, affecting approximately 1.4 million Americans.[1] IBDs are characterized by colon or small intestine inflammation and a relapsing course with clinically quiescent periods followed by bouts of severe and damaging inflammation associated with tissue destruction and mucosal erosion.[1] Apoptotic and necrotic features are often found in the crypt compartment of the affected intestinal tissue.[2] IBD etiology depends on genetic susceptibility and environmental triggers.[3] Although most research efforts have focused on immune cells, it is becoming increasingly clear that intestinal epithelial cells (IEC) are also important players in IBD pathogenesis[4] and their ability to regenerate and heal the injured mucosa is critical for long-term remission.[5] Interestingly, single nucleotide polymorphisms in ubiquitously expressed genes encoding nuclear factor (NF)-κB-regulated molecules show strong association with IBD[3,6] and activated/nuclear NF-κB is present in both IEC and lamina propria macrophages of active disease areas.[7] NF-κB stimulates transcription of numerous genes implicated in IBD pathogenesis, including *TNF*, which codes for the prototypical inflammatory cytokine tumor necrosis factor (TNF). TNF inhibition is one of the main therapeutic options in IBD[7] leading to reduced IEC apoptosis and enhanced mucosal repair.[8] Unlike other TNF-dependent inflammatory diseases, such as psoriasis, extensive epithelial cell death is a cardinal feature of IBD, yet the basis for TNF-induced IEC death is unknown, because TNF is not cytotoxic to normal IEC unless treated with protein synthesis inhibitors.

In fact, in most cell types, IEC included, transient TNF signaling inhibits apoptosis because of IKKβ-dependent NF-κB activation.[9] Correspondingly, ablation of IKKβ[10,11] or its regulatory subunit IKKγ/NEMO[12] renders IEC susceptible to TNF-induced death. Elevated expression of A20, a protein thought to be a negative regulator of NF-κB, also sensitizes IEC to TNF-mediated killing but this effect is not due to NF-κB inhibition.[13] Indeed, IKK or NF-κB deficiencies have not been described in IBD.

To determine whether persistent NF-κB activation in IBD[7] has a pathogenic function, we generated $Ikk\beta(EE)^{IEC}$ mice in which a constitutively active IKKβ(EE) variant is expressed in IEC from the villin promoter.[14] Surprisingly, instead of being resistant to TNF-induced mucosal erosion, $Ikk\beta(EE)^{IEC}$ mice display severe TNF-dependent epithelial layer destruction when challenged with TNF or various stimuli that induce TNF production.[14] The mechanism by which constitutive IKKβ/NF-κB activation renders mouse IEC susceptible to TNF-induced killing, rather than prevent it, is unknown, but is likely to be relevant to the effect of chronic NF-κB activation in IEC of active IBD lesions. We have therefore investigated the mechanisms by which TNF induces IEC death in $Ikk\beta(EE)^{IEC}$ mice.

We focused our studies on the function of RIPK1, a protein kinase that serves as a key regulator of life and death in TNF-exposed cells. Under conditions in which RIPK1 is subject to K63-linked and linear ubiquitination, TNFR1 engagement induces cell survival, but when the RIPK1 ubiquitination pattern is altered, TNF induces 1 of 2 forms of programmed cell death: necroptosis[15,16] or noncanonical apoptosis that is not inhibited by NF-κB.[17] The latter depends on formation of a RIPK1-dependent signaling complex that also contains FADD and caspase-8, known as complex IIb or the ripoptosome.[17] However, in cells that are completely deficient of RIPK1, which is needed for NF-κB activation,[18] TNF leads to a classical apoptotic response that is NF-κB preventable.[19–21] Adding to the complexities of TNF-mediated cell death and its dependence on NF-κB inhibition or RIPK1 kinase activation, we found that elevated A20 expression facilitates ripoptosome formation and RIPK1 activation.[13] Here we describe the role of RIPK1 in TNF-mediated IEC killing and mucosal erosion in $Ikk\beta(EE)^{IEC}$ mice.

Results

NF-κB and Caspase-3 Activation in Human IBD

We conducted immunohistochemistry (IHC) analysis of human tissue specimens from healthy individuals and patients suffering with either ileal or colonic CD or UC to determine the correlation between NF-κB activation and cell death. As previously described,[13] we examined 10 normal colon specimens, 10 samples with active UC, and 10 samples with colonic CD, as well as 4 active ileitis samples and 5 inactive ileal CD samples, all of which were stained for p65/RelA and cleaved caspase-3 (cC-3). In general, normal colonic or ileal specimens contained hardly any IEC that were positive for cC-3 or nuclear p65 (Figure 1*A*). As described,[13] active IBD specimens contained more cC-3-positive cells than control samples. Interestingly, the areas enriched for cC-3-positive cells

[a]Both authors contributed equally to this work.

Abbreviations used in this paper: **BHA, butylated hydroxyanisole; cC-3, cleaved caspase-3; cC-8, cleaved caspase-8; CD, Crohn's disease; CHX, cycloheximide; DPI, phenyleneiodonium; IB, immunoblotting; IBD, inflammatory bowel disease; IEC, intestinal epithelial cell; IHC, immunohistochemistry; i.p., intraperitoneally; LPS, lipopolysaccharide; Nec-1, necrostatin-1; NF, nuclear factor; PBS, phosphate-buffered saline; qPCR, quantitative polymerase chain reaction; TNF, tumor necrosis factor; UC, ulcerative colitis; WT, wild type.**

Most current article

2352-345X
https://doi.org/10.1016/j.jcmgh.2019.10.002

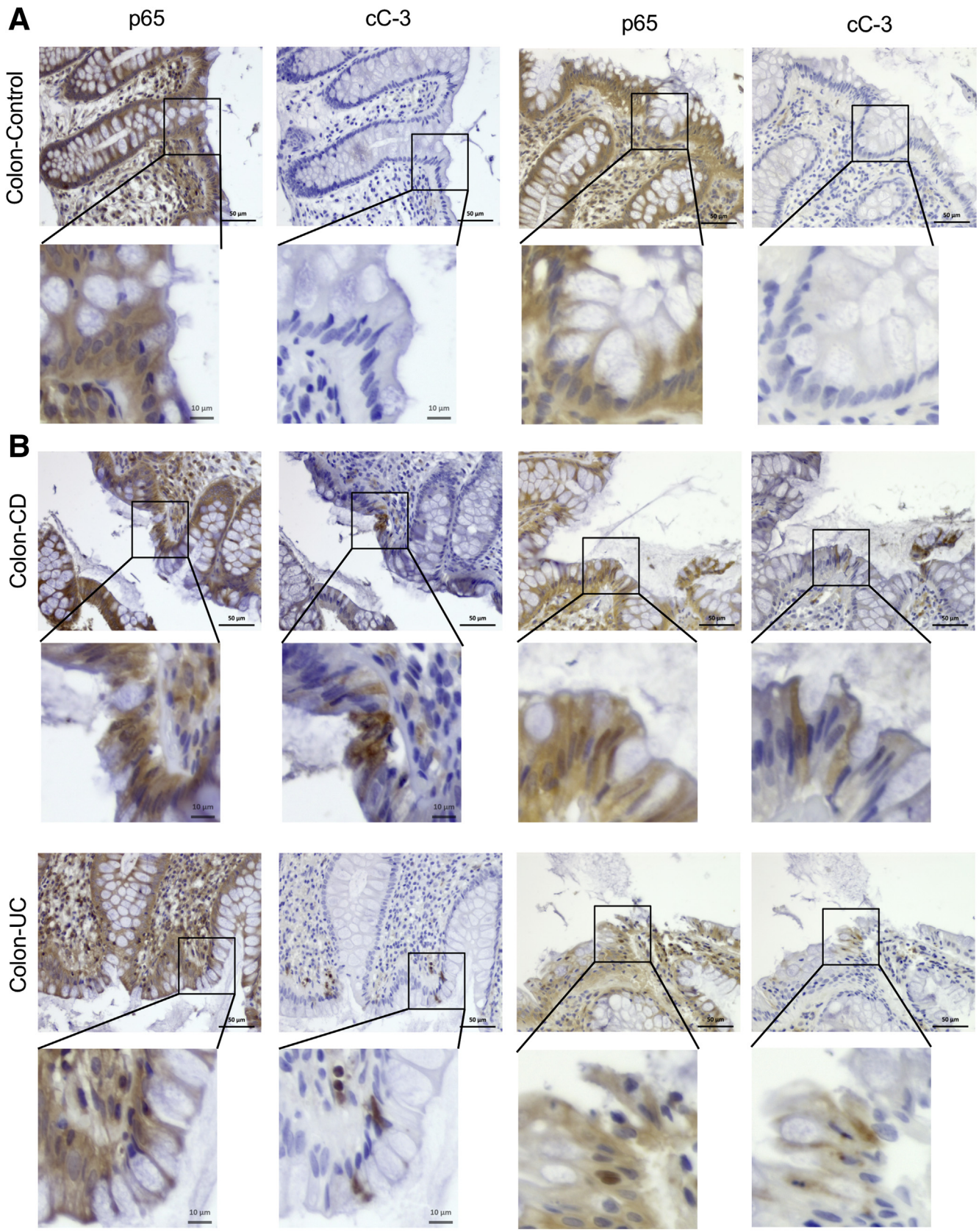

Figure 1. Active IBD tissue displays spatially adjacent NF-κB and caspase-3 activation in intestinal epithelial cells. Human control (*A*), CD and UC colon sections (*B*) were stained with antibodies to cC-3 and p65(RelA). Magnification bars: 50 μm. *Arrows* show positive cells. Results are representative for 15 healthy, 14 CD, and 10 UC specimens.

Table 1. Number of Samples and the Corresponding Percentages of Nuclear p65 and Cleaved Caspase 3 Expression Level in IEC of Control Tissue and Active IBD Specimens

Expression level	C ileum	C colon	CD ileum	CD colon	UC colon
Nuclear p65 expression level					
0	4 (80)	7 (70)	1 (25)	0	0
1	1 (20)	3 (30)	1 (25)	2 (20)	1 (10)
2	0	0	2 (50)	5 (50)	4 (40)
3	0	0	0	3 (30)	5 (50)
Total	5	10	4	10	10
Caspase-3 expression level					
0	2 (40)	5 (50)	1 (25)	0	0
1	3 (60)	5 (50)	1 (25)	3 (30)	2 (20)
2	0	0	2 (50)	5 (50)	4 (40)
3	0	0	0	2 (20)	4 (40)
Total	5	10	4	10	10

C, control; CD, Crohn's disease; IBD, inflammatory bowel disease; IEC, intestinal epithelial cells; UC, ulcerative colitis.

correlated with areas harboring cells with nuclear p65 (Figure 1*A* and *B*). Active UC specimens contained more cC-3- and p65-positive cells than CD specimens and hardly any differences were observed between colonic and ileal CD (Table 1). Our finding of activated/nuclear NF-κB in IEC is consistent with other reports.[7,22] In addition, mining of publicly available data sets also showed upregulation of numerous NF-κB target genes including *TNFAIP3*, *CXCL10*, *CXCL11*, *CCL2*, *CCL8*, *CSF1*, *CCL11*, and *CCL20* in active IBD areas that decreased after anti-TNF therapy (Figure 2*A*).[23]

TNF-Induced Apoptosis in Ikkβ(EE)^{IEC} *Mice*

To determine the pathogenic function of persistent NF-κB activation we used *Ikkβ(EE)^{IEC}* mice, which instead of being resistant to TNF-induced mucosal erosion are highly sensitive to TNF.[14] Of note, many of the genes found to be up-regulated in human IBD and described in our previous work[13] were also up-regulated in *Ikkβ(EE)^{IEC}* mice relative to the wild-type (WT) mouse epithelium (Figure 2*B*).[14]

Because TNF can trigger either apoptosis or necroptosis, we used IHC with antibodies specific for activated/cleaved caspase-8 (cC-8) or cC-3 to determine the type of cell death affecting the *Ikkβ(EE)^{IEC}* small bowel epithelium after administration of TNF or lipopolysaccharide (LPS). Treatment of *Ikkβ(EE)^{IEC}* mice with either agent activated both caspases (Figure 3*A* and *B*). TNF-treated WT mice showed only a mild and transient caspase-3 activation near the villi tips, but not within the crypt compartment, and hardly any caspase-8 activation, correlating with little or no mucosal damage. TNF-treated *Ikkβ(EE)^{IEC}* mice, however, displayed activation of both caspases in villi and especially within crypt compartments, leading to cell shedding and tissue damage (0.02 $\pm$ 0.03 cC-3$^+$ and 0.01 $\pm$ 0.02 cC-8$^+$ cells per crypt in WT vs 7.01 $\pm$ 1.15 cC-3$^+$ and 4.35 $\pm$ 2.19 cC-8$^+$ cells per crypt in *Ikkβ(EE)^{IEC}* mice; $P < .001$ and $P < .001$). Immunoblotting (IB) analysis of the intestinal crypt fraction of *Ikkβ(EE)^{IEC}* mice intraperitoneally (i.p.) injected with LPS showed strong and sustained cleavage of caspases-3 and -8 and delayed degradation of IKKβ(EE) protein, likely because of caspase activation (Figure 3*B*). As described,[14] *Ikkβ(EE)^{IEC}/Tnf$^{-/-}$* mice remained hypersensitive to exogenous TNF and showed caspase-3 and -8 activation after its administration (6.99 $\pm$ 1.50 cC-3$^+$ and 3.38 $\pm$ 0.59 cC-8$^+$ cells per crypt in *Ikkβ(EE)^{IEC}* vs 5.07 $\pm$ 0.78 cC-3$^+$ and 1.93 $\pm$ 0.61 cC-8$^+$ cells per crypt in *Ikkβ(EE)^{IEC}/Tnf$^{-/-}$* mice; $P = .015$ and $P < .001$) (Figure 3*C*). Similar results were obtained in TNF-treated *Ikkβ(EE)^{IEC}/Myd88$^{\Delta IEC}$* mice (5.72 $\pm$ 2.22 cC-3$^+$ and 4.35 $\pm$ 1.12 cC-8$^+$ cells per crypt in *Ikkβ(EE)^{IEC}/Myd88$^{F/F}$* mice vs 8.18 $\pm$ 1.17 cC-3$^+$ and 5.61 $\pm$ 0.76 cC-8$^+$ cells per crypt in *Ikkβ(EE)^{IEC}/Myd88$^{\Delta IEC}$* mice; $P = .015$ and $P = .02$) (Figure 3*D*), suggesting an inherent ability of persistent IKKβ activation to sensitize IEC to TNF-induced apoptosis independently of IEC-autonomous toll-like receptor signaling.

To further investigate this phenomenon and determine whether or not it depends on microbiota and immune cells, we established enteroid cultures.[24] Whereas WT enteroids exhibited minimal TNF-induced death, *Ikkβ(EE)^{IEC}* and *Ikkβ(EE)^{IEC}/Tnf$^{-/-}$* enteroids underwent extensive cell death, especially within crypt domains, after incubation with TNF (1.9% $\pm$ 3.8% WT dead organoids vs 95.5% $\pm$ 5.4% dead in *Ikkβ(EE)^{IEC}* organoids; $P < .001$) (Figure 4*A* and *B*), leading to their rapid disintegration. cC-3 and TUNEL immunofluorescent staining (Figure 4*C* and *D*) and IB analysis of caspases-3 and -8 (Figure 4*E* and *F*) correlated and confirmed that *Ikkβ(EE)^{IEC}* or *Ikkβ(EE)^{IEC}/Tnf$^{-/-}$* enteroids underwent TNF-induced apoptosis mainly within crypt domains. Inducible expression of IKKβ(EE) in WT enteroids also conferred susceptibility to TNF-induced apoptosis (Figure 5*A*). Doxycycline, which was used to induce IKKβ(EE) expression, did not cause cell death, neither did it sensitize WT enteroids to TNF-induced apoptosis (Figure 5*B*).

To determine whether the elevated susceptibility of *Ikkβ(EE)^{IEC}* enteroids to TNF-induced death was NF-κB-dependent, we transduced them with a lentivirus expressing IκBα super-repressor (IκBαSR). Enteroids containing IκBαSR no longer exhibited TNF-induced crypt apoptosis (Figure 5*C*), but unexpectedly IkBαSR expression led to reduced IKKβ(EE) expression (Figure 5*D*).

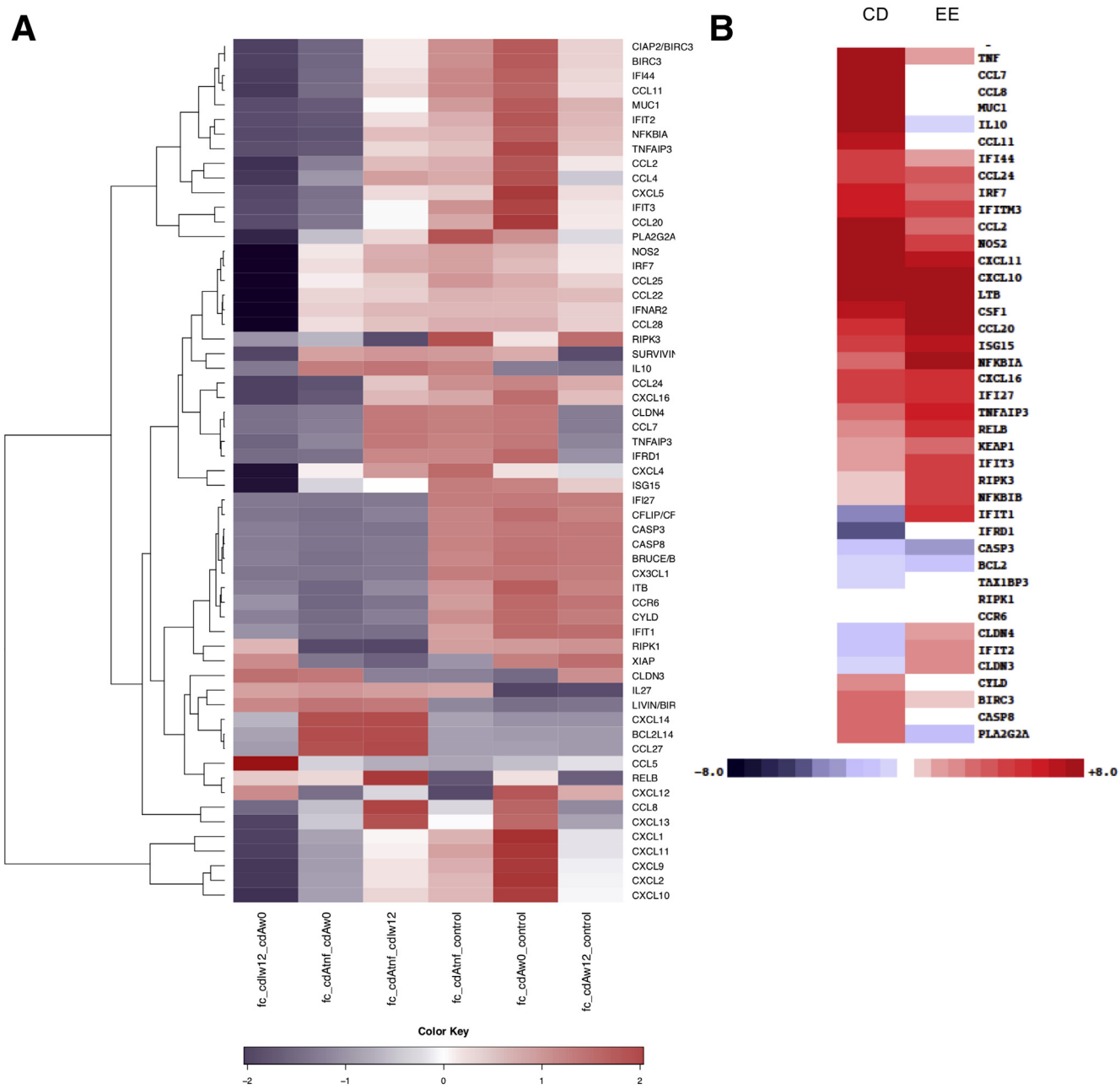

Figure 2. Anti-TNF treatment decreases expression of NF-κB-related genes in human IBD tissue. (*A*) Heat map showing differentially expressed NF-κB-related genes between healthy control subjects and CD subjects, before and after anti-TNF therapy, in tissue biopsies described in array GSE52746.[23] Fc_cdIw12_cdAw0 means fold-change between CD samples from inactive areas after 12 weeks of anti-TNF therapy and CD samples from active areas at time 0; fc_cdAtnf_cdAw0 means fold-change between CD samples from active areas after 12 weeks of anti-TNF therapy and CD samples from active areas at time 0; fc_cdAtnf_cdIw12 means fold change between CD samples from active areas after 12 weeks of anti-TNF therapy and CD samples from inactive areas after 12 weeks of anti-TNF therapy; fc_cdAtnf_control means fold change between CD samples from active areas after 12 weeks of anti-TNF therapy and healthy control samples; fc_cdAw0_control means fold change between CD samples from active areas at time 0 and healthy control samples; fc_cdAw12_control means fold change between CD samples from active areas after 12 weeks of anti-TNF therapy and healthy control samples. (*B*) Comparison between genes that are differentially expressed between WT and *Ikkβ(EE)*^{IEC} enterocytes[14] and those that are differentially expressed between CD and normal human ileum (*left*).[13]

RIPK1 Kinase Activity Is Required for TNF-Induced Tissue Damage

TNFR1 engagement triggers assembly of several distinct signaling complexes, the first of which is complex I, which includes TRADD, RIPK1, TRAF2, and cIAP1/2, and is responsible for IKK and NF-κB activation and inhibition of apoptosis. The latter is mediated by induction of anti-apoptotic genes, including those coding for c-FLIP, a

caspase-8 inhibitor,[25] and survivin, a caspase-3 inhibitor.[26] Complex I formation and NF-κB activation depend on the scaffold functions of RIPK1 but not on its kinase activity.[16] Notably, and despite its susceptibility to TNF-induced apoptosis, the intestinal epithelium of *Ikkβ(EE)*^{IEC} mice exhibited elevated expression of antiapoptotic molecules,

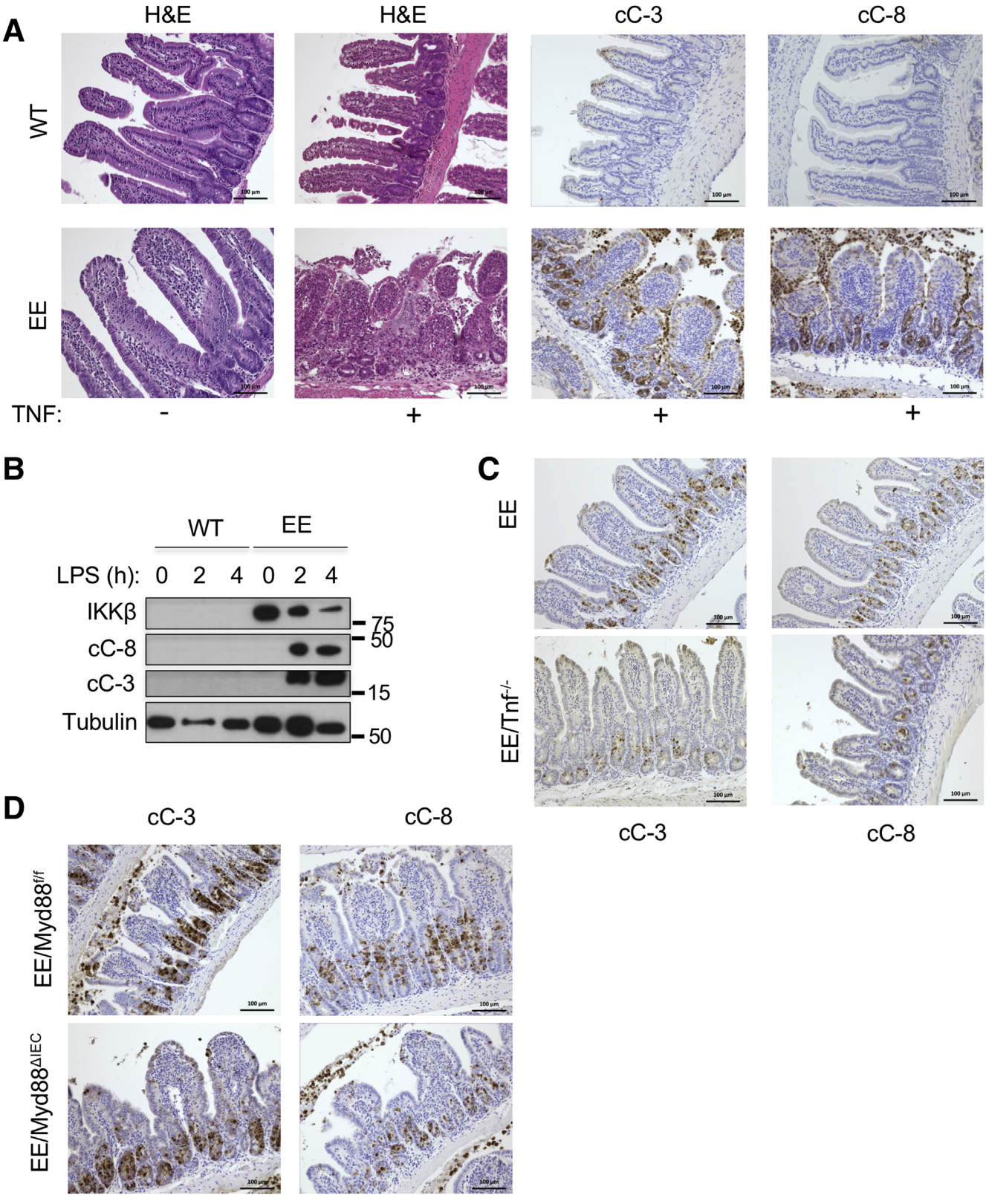

including BIRC3, BCL2, and BCL2L1.[14] Persistent TNFR1 engagement, however, results in receptor internalization, which can promote cell death through either RIPK1 kinase-dependent apoptosis or necroptosis.[16,27] To query the involvement of RIPK1 kinase activity in the observed response of *Ikkβ(EE)^{IEC}* enteroids, we examined the ability of necrostatin-1 (Nec-1), a RIPK1 inhibitor,[28] to block TNF-induced killing. Indeed, Nec-1 effectively blocked TNF-induced *Ikkβ(EE)^{IEC}* enteroid apoptosis (Figure 6*A* and *B*), without any effect on crypt proliferation (Figure 6*C* and *D*). Nec-1, however, can also inhibit other kinases, such as PAK1.[29] We therefore examined the effect of more specific RIPK1 kinase inhibitors and inhibitors of RIPK3, a key inducer of necroptosis.[30,31] The RIPK1 inhibitors (GSK'963 and GSK'728 or Nec-1s, which is the active enantiomer of the optimized necrostatin 7-Cl-O-Nec-1), but not the RIPK3 selective inhibitors (GSK'843 and GSK'872), prevented the TNF-induced death of *Ikkβ(EE)^{IEC}* intestinal enteroids and blocked caspase-3 and -8 cleavage (95.5% ± 5.4% dead organoids after control treatment vs 2.8% ± 3.3% after Nec-1, 3.0% ± 3.5% after GSK'963, 4.9% ± 0.5% after Nec-1s, 95.7% ±5.8% after GSK'843, and 97.7% ± 4.5% after GSK'872 treatments) (Figure 6*A* and *B*).

To further validate the role of RIPK1 in TNF-induced apoptosis and tissue damage in *Ikkβ(EE)^{IEC}* mice, we crossed the latter to *Ripk1$^{D138N/D138N}$* homozygous knockin mice, which express a catalytically inactive version of RIPK1 that retains its scaffold function.[32] We also crossed *Ikkβ(EE)^{IEC}* mice with *Rip3$^{-/-}$* mice[33] to genetically rule out a role for RIPK3-dependent necroptosis in TNF-induced mucosal erosion in our model. Notably, *Ripk3* ablation did not prevent TNF-induced apoptosis (Figure 7*A* and *B*) but RIPK1 kinase inactivation completely blocked TNF-induced crypt cell death and caspase-3 activation in *Ikkβ(EE)^{IEC}* enteroids (95.5% ± 5.4% dead *Ikkβ(EE)^{IEC}* organoids vs 2.0% ± 4.0% dead *Ikkβ(EE)^{IEC}/Ripk1$^{D138N/D138N}$* organoids) (Figure 7*C* and *D*). As expected,[34,35] *Ripk3* gene ablation prevented necroptosis in enteroids incubated with TNF + cycloheximide (CHX) + zVAD (5.59 ± 3.12 cC-3$^+$ cells per crypt in *Ikkβ(EE)^{IEC}* mice vs 6.79 ± 1.02 cC-3$^+$ cells per crypt in *Ikkβ(EE)^{IEC}/Rip3$^{-/-}$* mice; $P = .91$) (Figure 7*E* and *F*).

Ikkβ(EE)^{IEC} mice are highly sensitive to TNF-induced mucosal damage and even a low dose of LPS, which induces TNF expression, causes their rapid death.[14] Whereas *Ripk3* ablation did not decrease LPS-induced mortality, or LPS-induced caspase-3 or -8 activation (not shown) in *Ikkβ(EE)^{IEC}* mice (Figures 4*A* and 5*D*), RIPK1 inactivation was fully protective (Figure 8*A* and *B*). RIPK1 inactivation also inhibited TNF- and LPS-induced caspase-3 activation in *Ikkβ(EE)^{IEC}* intestinal villi and crypts (5.25 ± 1 cC-3$^+$ cells per crypt in *Ikkβ(EE)^{IEC}* vs 1.1 ± 0.35 cC-3$^+$ cells in *Ikkβ(EE)^{IEC}/Ripk1$^{D138N/D138N}$* mice, 4 hours after LPS administration; $P < .001$), as assessed by IHC (Figure 8*C*). Furthermore, the specific RIPK1 inhibitor GSK'963 prevented LPS-induced tissue damage, apoptosis (5.5 ± 0.3 cC-3$^+$ cells per crypt in *Ikkβ(EE)^{IEC}* mice vs 3.2 ± 0.6 cC-3$^+$ cells in GSK'963-treated *Ikkβ(EE)^{IEC}* mice; $P = .002$) and death in *Ikkβ(EE)^{IEC}* mice challenged with LPS (Figure 8*B* and *D*). Curiously, within 1 hour after TNF or LPS administration, WT mice contained a few cC-3$^+$ IEC in their villi, whose number was also reduced on RIPK1 inactivation (4.5 ± 0.8 cC-3$^+$ cells per villus in WT mice vs 1.5 ± 0.5 cC-3$^+$ cells per villus in *Ripk1$^{D138N/D138N}$* mice; $P = .01$) (Figure 8*C*).

Ripoptosome Formation and Protection by Antioxidants

RIPK1 activation as a kinase and RIPK1-dependent apoptosis depend on formation of the ripoptosome, or complex IIb, which also contains FADD, A20, and caspase-8.[13,17,36] We have recently shown that A20 overexpression in IECs induces ripoptosome formation and activation in response to TNF.[13] Because A20 expression is elevated in IKKβ(EE)-expressing IEC (Figures 9*A* and 2*B*) we examined its role in TNF-induced *Ikkβ(EE)^{IEC}* enteroid death by crossing *Ikkβ(EE)^{IEC}* mice with A20$^{\Delta IEC}$ mice, which specifically lack A20 in IEC.[13] We then infected IKKβ(EE)/A20$^{\Delta IEC}$ enteroids with a doxycycline inducible vector coding for either WT A20 or an A20 variant with a C764A/C767A double substitution that impairs the linear ubiquitin binding ability of zinc finger 7 (A20^{ZNF7mut}), which is needed for RIPK1 activation.[13] As expected, TNF induced caspase activation in IKKβ(EE)/A20$^{\Delta IEC}$ (29930103). Surprisingly, expression of the protective A20^{ZNF7mut} did not prevent caspase-3 and -8 activation as effectively as WT A20 (Figure 9*B*), demonstrating that A20 upregulation is not responsible for TNF-induced apoptosis in *Ikkβ(EE)^{IEC}* IEC.

Previous studies have shown that RIPK1 activation increases reactive oxygen species production after TNF stimulation[37] to potentiate RIPK1-dependent cell death.[38,39] We therefore examined the effect of the antioxidant butylated hydroxyanisole (BHA), which was shown to inhibit ripoptosome formation,[38] on TNF-mediated apoptosis and caspase activation in *Ikkβ(EE)^{IEC}* enteroids. Consistent with previous reports, BHA, but not diphenyleneiodonium (DPI), a NOX inhibitor, fully prevented TNF-induced apoptosis and caspase activation (95.5% ± 5.4% dead organoids after control treatment vs 23.7% ± 20.0% dead organoids after BHA or 97.9% ± 4.1% after DPI treatment) (Figure 9*C* and *D*). BHA treatment also inhibited

Figure 3. (*See previous page*). IKKβ(EE)-expressing intestinal crypts are highly susceptible to TNF-induced apoptosis independently of toll-like receptor signaling. (*A*) WT and *Ikkβ(EE)^{IEC}* mice were analyzed 4 hours after TNF injection (2 μg intravenously). Jejunal sections were stained with either H&E or antibodies to cC-3 or cC-8. Magnification bars: 100 μm. (*B*) Lysates of WT and *Ikkβ(EE)^{IEC}* intestinal mucosa were analyzed at different times after LPS injection (5 mg/kg) by IB. (*C*) *Ikkβ(EE)^{IEC}* and *Ikkβ(EE)^{IEC}/Tnf$^{-/-}$* mice were injected with TNF (2 μg intravenously). Jejunal sections were prepared 4 hours later and stained with antibodies to either cC-3 or cC-8. Magnification bars: 100 μm. (*D*) *Ikkβ(EE)^{IEC}/Myd88$^{\Delta IEC}$* and *Ikkβ(EE)^{IEC}/Myd88$^{F/F}$* mice were analyzed 4 hours after TNF injection as above.

ripoptosome-mediated caspase-8 activation, assessed by caspase-8 coprecipitation with FADD, almost as effectively as Nec-1 (Figure 9*E*). Accordingly, BHA administration to *Ikkβ(EE)*^{IEC} mice abrogated LPS-induced mortality and IEC apoptosis (5.85 ± 1.04 cC-3^{+} and 3.01 ± 0.83 cC-8^{+} cells per crypt after control treatment vs 0.00 ± 0.00 cC-3^{+} and 0.00 ± 0.00 cC-8^{+} cells per crypt in BHA-treated mice; $P <$ .001 and $P <$ .001) (Figure 9*F* and *G*).

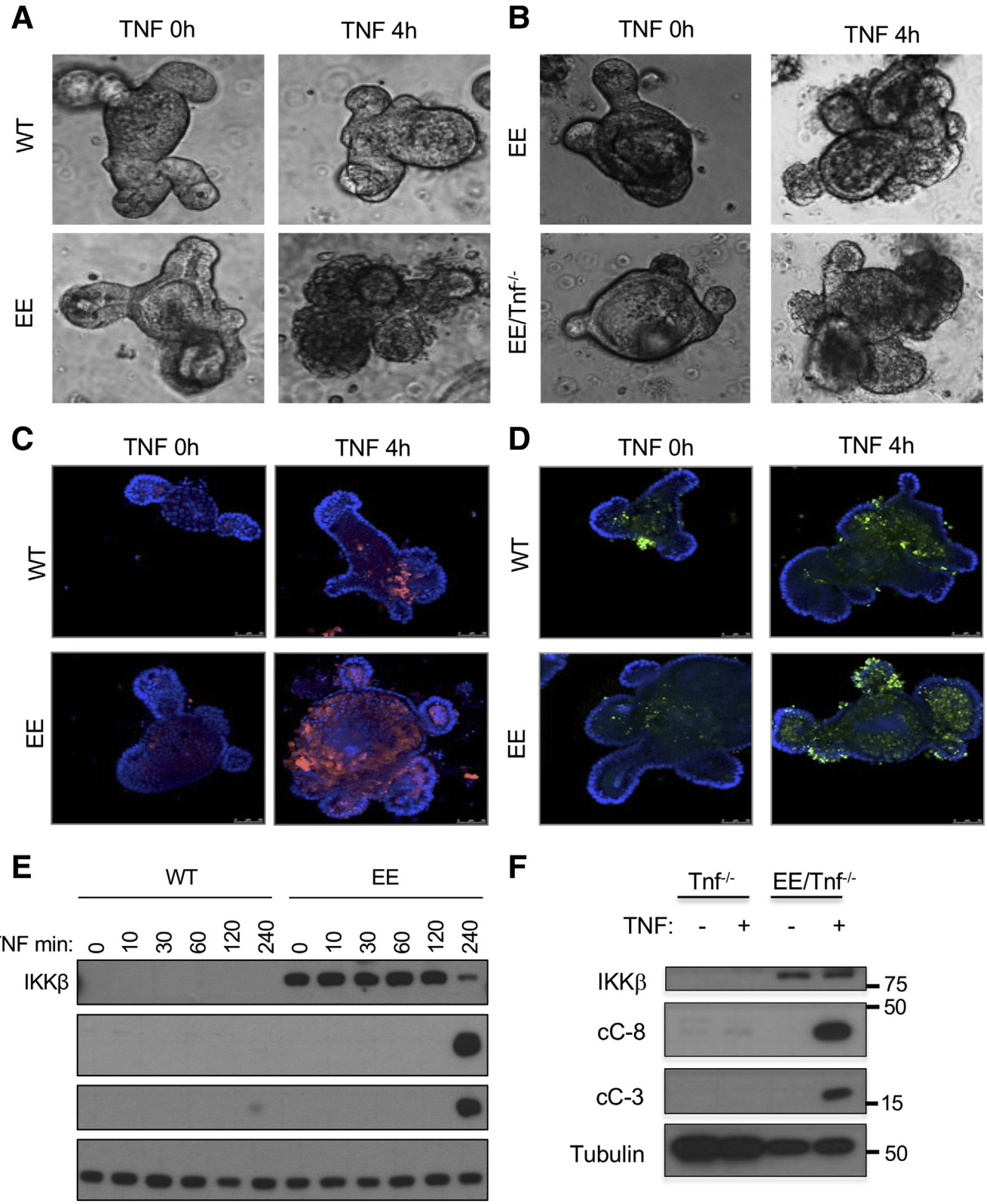

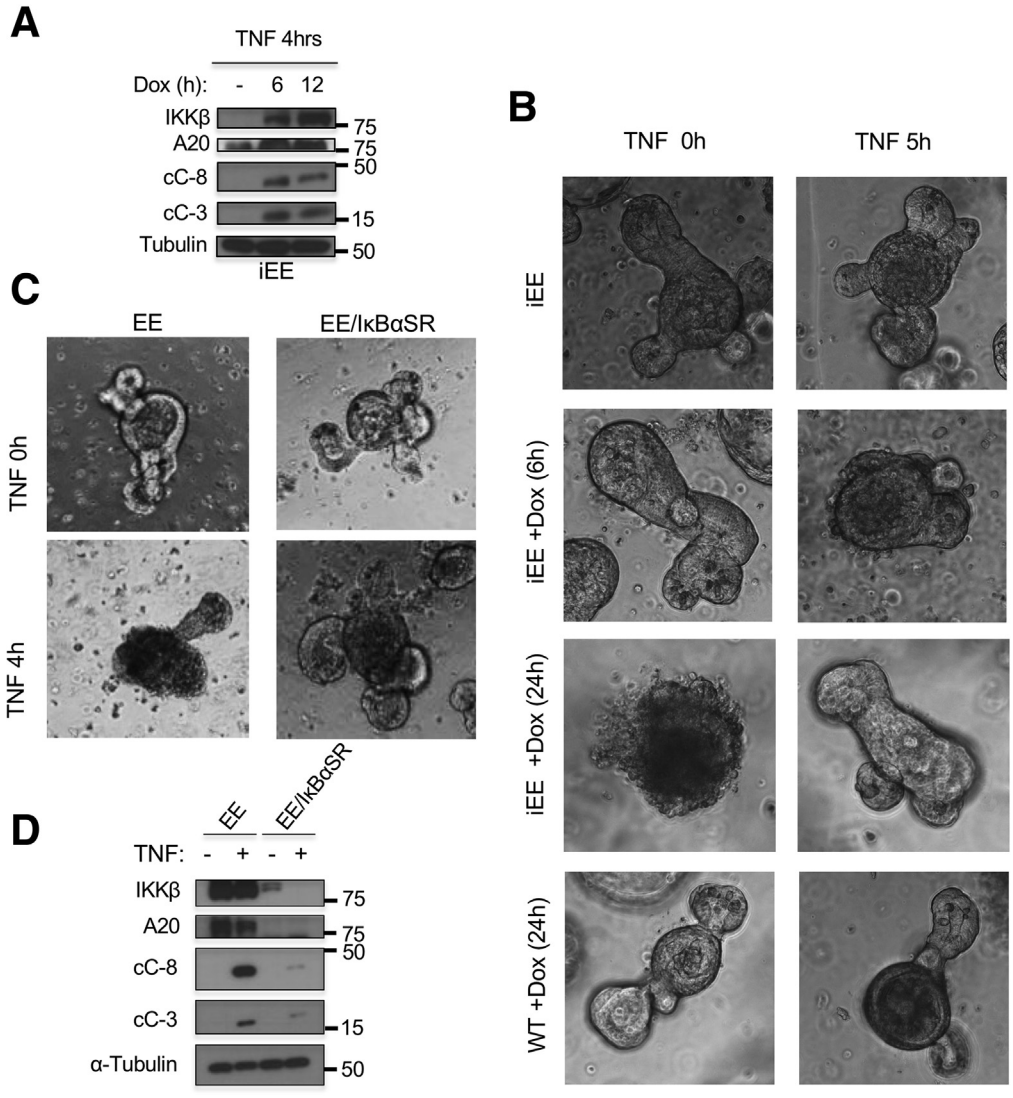

Figure 5. Susceptibility of *Ikkβ(EE)^{IEC}* enteroids to TNF-induced death is NF-κB-dependent. (*A*) WT enteroids transduced with an inducible IKKβ(EE) construct were pre-incubated with or without doxycycline as indicated, lysed, and IB analyzed 4 hours after TNF addition. (*B*) Control and inducible-IKKβ(EE) transduced WT enteroids were incubated for 24 hours with doxycycline before TNF stimulation as indicated. Original magnification X200. (*C*) Control and IκBαSR-transduced *Ikkβ(EE)^{IEC}* enteroids were incubated with TNF as indicated and photographed under bright field. Original magnification ×200. (*D*) Control and IκBαSR-transduced *Ikkβ(EE)^{IEC}* enteroids incubated with or without TNF were lysed and IB analyzed.

Discussion

TNF is a major pathogenic factor in IBD and its blockade represents one of the most effective therapeutic options for these diseases. However, how TNF triggers IEC killing and mucosal erosion has remained a mystery. Although certain genetic mutations associated with IBD, such as ATGL1^{T300A}, increase IEC susceptibility to TNF[3,40–42] and several studies have identified, in different ethnic cohorts, 235 genetic markers in 200 susceptibility loci, some of them involving the NF-κB pathway, such as TNFAIP3 and NFKB1,[3,43–45] TNF is a poor killer of normal IEC and can promote antiapoptotic NF-κB activation.[11] Not surprising, NF-κB-deficient IEC are highly susceptible to TNF-induced killing, which depends on conventional, caspase-8-dependent, apoptosis.[10–12,46] However, rather unexpectedly, we found that excessive IKKβ-mediated NF-κB activation reduces the threshold needed for induction of TNF-induced IEC death.[14] Here we show that the TNF

Figure 4. (*See previous page*). TNF induces apoptosis in IKKβ(EE)-expressing intestinal enteroids. (*A*) WT and *Ikkβ(EE)^{IEC}* enteroids were photographed under brightfield 4 hours after TNF stimulation (40 ng/mL). Original magnification ×200. (*B*) *Ikkβ(EE)^{IEC}* and *Ikkβ(EE)^{IEC}/Tnf$^{-/-}$* enteroids were photographed under brightfield before and after incubation with TNF (40 ng/mL). Original magnification ×200. (*C*) WT and *Ikkβ(EE)^{IEC}* enteroids were stained with cC-8 antibody and visualized by confocal microscopy at the indicated times after TNF (40 ng/mL) addition. Magnification bars: 100 μm. (*D*) WT and *Ikkβ(EE)^{IEC}* enteroids were TUNEL stained and analyzed by confocal microscopy before and after incubation with TNF. Apoptotic cells are *bright green*. Magnification bars: 100 μm. (*E*) Lysates of WT and *Ikkβ(EE)^{IEC}* enteroids were IB analyzed at different times after TNF addition. (*F*) Lysates of *Tnf$^{-/-}$* and *Ikkβ(EE)^{IEC}/Tnf$^{-/-}$* enteroids incubated with or without TNF were analyzed for caspase activation by IB.

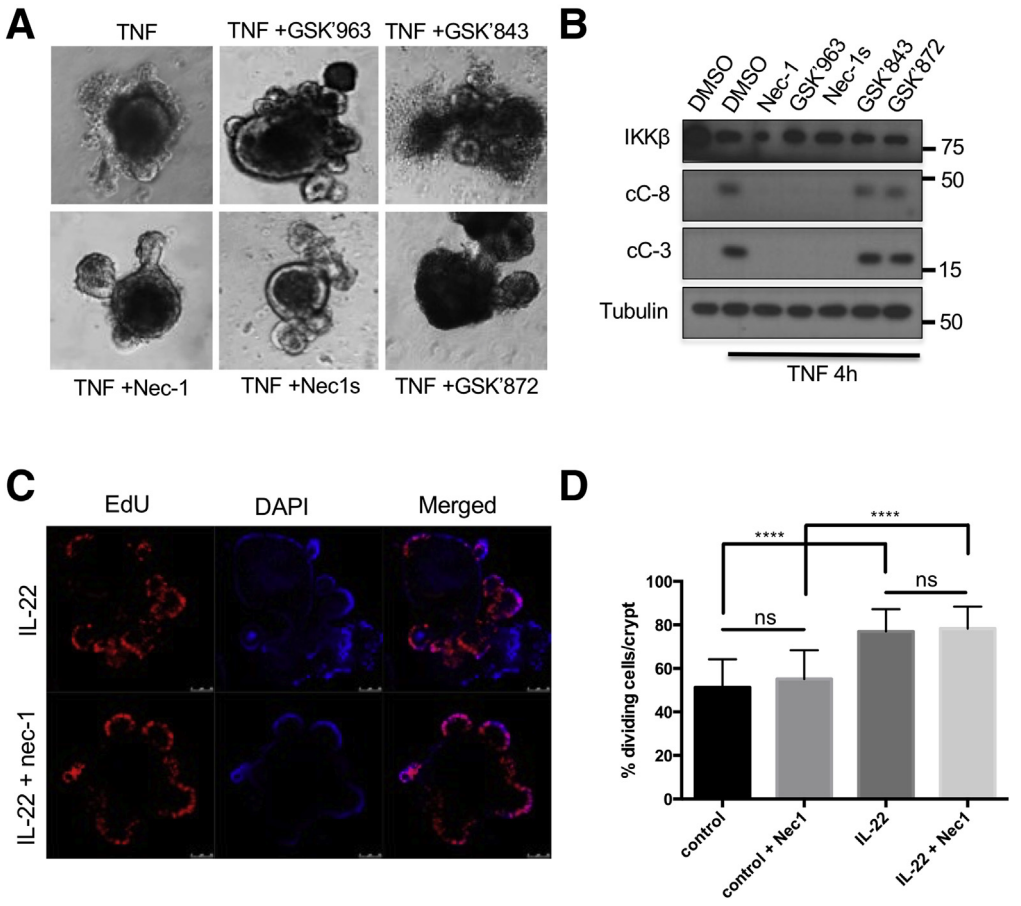

Figure 6. RIPK1 kinase activity is required for TNF-induced enteroid death. (*A*) *Ikkβ(EE)*^{IEC} enteroids were incubated with TNF (40 ng/mL) in the absence or presence of RIPK1 or RIPK3 inhibitors and photographed 4 hours later. Original magnification ×200. (*B*) Lysates of *Ikkβ(EE)*^{IEC} enteroids treated as above were subjected to IB analysis after 4 hours. (*C*) WT enteroids were treated for 24 hours with interleukin-22 (10 ng/mL) in the absence or presence of Nec-1. Two hours before fixation, EdU was added to the culture medium. ****$P \leq .0001$. (*D*) Percentages of EdU positive cells per crypt are shown. IL, interleukin; ns, not significant.

induced death of IKKβ(EE)-expressing IEC depends on RIPK1 kinase activation and presumably ripoptosome formation.

TNF-induced ripoptosome formation in IEC and RIPK1-dependent apoptosis are also facilitated by elevated expression of the deubiquitinase A20.[13] Since expression of *TNFAIP3*, the gene coding for A20, is stimulated by NF-κB and is elevated in *Ikkβ(EE)*^{IEC} mice, a likely explanation to the reduced threshold for TNF-induced mucosal erosion and IEC death driven by IKKβ(EE) is A20. Although A20 ablation abrogated the TNF-induced death of IKKβ(EE)-expressing IEC, reconstitution of A20 expression with a variant, A20^{ZNF7mut}, that no longer enhances TNF-induced ripoptosome formation[13] led to full restoration of TNF-induced apoptosis. These results suggest that IKKβ(EE) expression overcomes the requirement for linear ubiquitin binding by the seventh ZnF of A20.[13] Exactly how IKKβ(EE) expression does that is not entirely clear, but our results show that its ability to reduce the threshold for TNF-induced death is NF-κB mediated. Because TNF-induced ripoptosome formation and RIPK1-mediated apoptosis in IKKβ (EE)-expressing IEC is inhibited by BHA, it is plausible that NF-κB activation may promote the accumulation of reactive oxygen species or other pro-oxidants. Curiously, oxidative stress is also thought to be involved in IBD pathogenesis,[47] and our results show that NF-κB is activated in active human IBD. Indeed, in previous studies we found that *Ikkβ(EE)*^{IEC} mice exhibit higher levels of oxidative DNA damage, which facilitates loss of *APC* heterozygocity to cause that formation of colonic adenomas and premalignant aberrant crypt foci,[48] a pathologic process that also occurs in patients with IBD.[49,50] It is also plausible that chronic NF-κB signaling affects Paneth cell differentiation or alters autophagy signaling, thereby increasing the susceptibility to TNF-induced cell death, in a similar manner to the effect of the *ATG16L1* or *NOD2* gene mutations.[51] Overall, our results suggest that RIPK1 inhibition and treatment with antioxidants may attenuate these pathologies, especially in conjunction with anti-TNF drugs.

Materials and Methods

Mice

Ikkβ(EE)^{IEC} and *Ripk1*^{D138N} mice were described.[14,32] *Ripk3*$^{-/-}$ mice were obtained from Dr. Vishva Dixit (Genentech).[52] *A20*$^{F/F}$ mice were obtained from Dr. Avril Ma.[53] *Ikkβ(EE)*^{IEC} mice were crossed to *Tnf*$^{-/-}$, *Ripk3*$^{-/-}$, and *Ripk1*$^{D138N/D138N}$ mice, and maintained in the C57BL/6J background originally acquired from Jackson Laboratories. Mice used in this work were 8–12 weeks old and were maintained under specific pathogen free (SPF) conditions at a University of California San Diego facility, accredited by

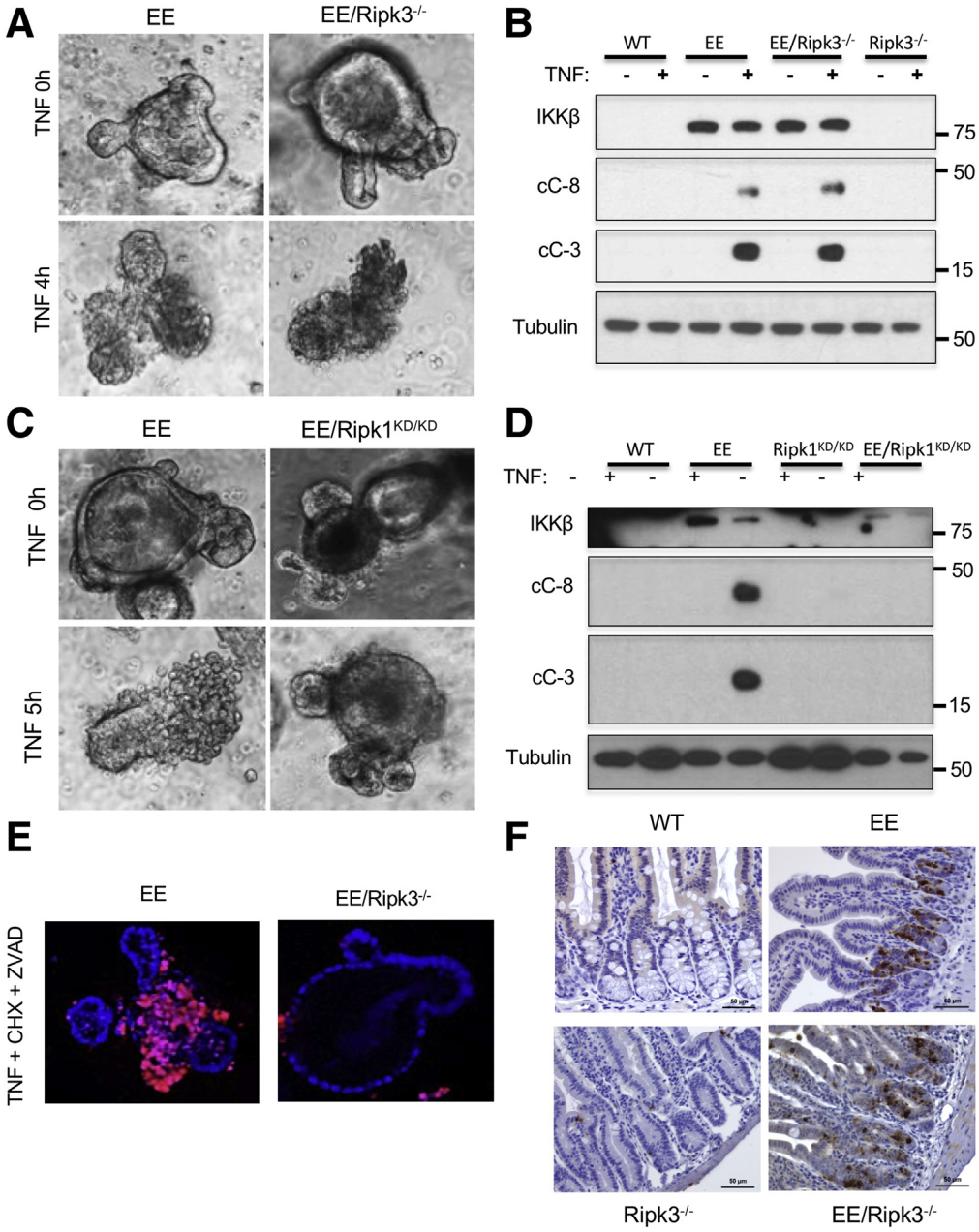

Figure 7. TNF-induced mucosal damage and IEC death is RIPK3-independent. (*A*) *Ikkβ(EE)^{IEC}* and *Ikkβ(EE)^{IEC}/Rip3$^{-/-}$* enteroids were photographed under brightfield before and 4 hours after incubation with TNF (40 ng/mL). Original magnification ×200. (*B*) WT, *Ikkβ(EE)^{IEC}*, *Rip3$^{-/-}$* and *Ikkβ(EE)^{IEC}/Rip3$^{-/-}$* enteroids were incubated with or without TNF, lysed, and IB analyzed 5 hours later. (*C*) *Ikkβ(EE)^{IEC}* and *Ikkβ(EE)^{IEC}/Ripk1$^{D138N/D138N}$* enteroids were photographed under brightfield before and 5 hours after TNF addition. Original magnification ×200. (*D*) WT, *Ikkβ(EE)^{IEC}*, *Ripk1$^{D138N/D138N}$*, and *Ikkβ(EE)^{IEC}/Ripk1$^{D138N/D138N}$* enteroids were incubated with or without TNF, lysed, and IB analyzed 5 hours later. (*E*) *Ikkβ(EE)^{IEC}* and *Ikkβ(EE)^{IEC}/Rip3$^{-/-}$* enteroids were incubated with TNF (40 ng/mL), CHX (25 μg/mL), and zVAD (10 μg/mL) for 4 hours, stained with Hoechst 33342 and propidium iodide and examined by confocal microscopy. Original magnification ×200. (*F*) WT, *Ikkβ(EE)^{IEC}*, *Rip3$^{-/-}$*, and *Ikkβ(EE)^{IEC}/Rip3$^{-/-}$* mice were analyzed 4 hours after LPS (0.5 μg/g i.p.) injection. Jejunal sections were stained with antibody to cC-3 and photographed. Magnification bars: 100 μm.

the American Association for Accreditation of Laboratory Animal Care. All animal protocols were approved by the institutional review board, following National Institutes of Health guidelines. Mice were fed autoclaved standard chow and all of the different strains were cohoused to minimize microbiome fluctuations.

Reagents

LPS (*Escherichia coli O111:B4*) was purchased from Sigma (St. Louis, MO) and was i.p. injected at 0.5 mg/kg, unless otherwise indicated. TNF was purchased from R&D systems (Minneapolis, MN) and injected at 2 μg per mouse unless otherwise indicated. *In vitro*, TNF was used at 40 ng/

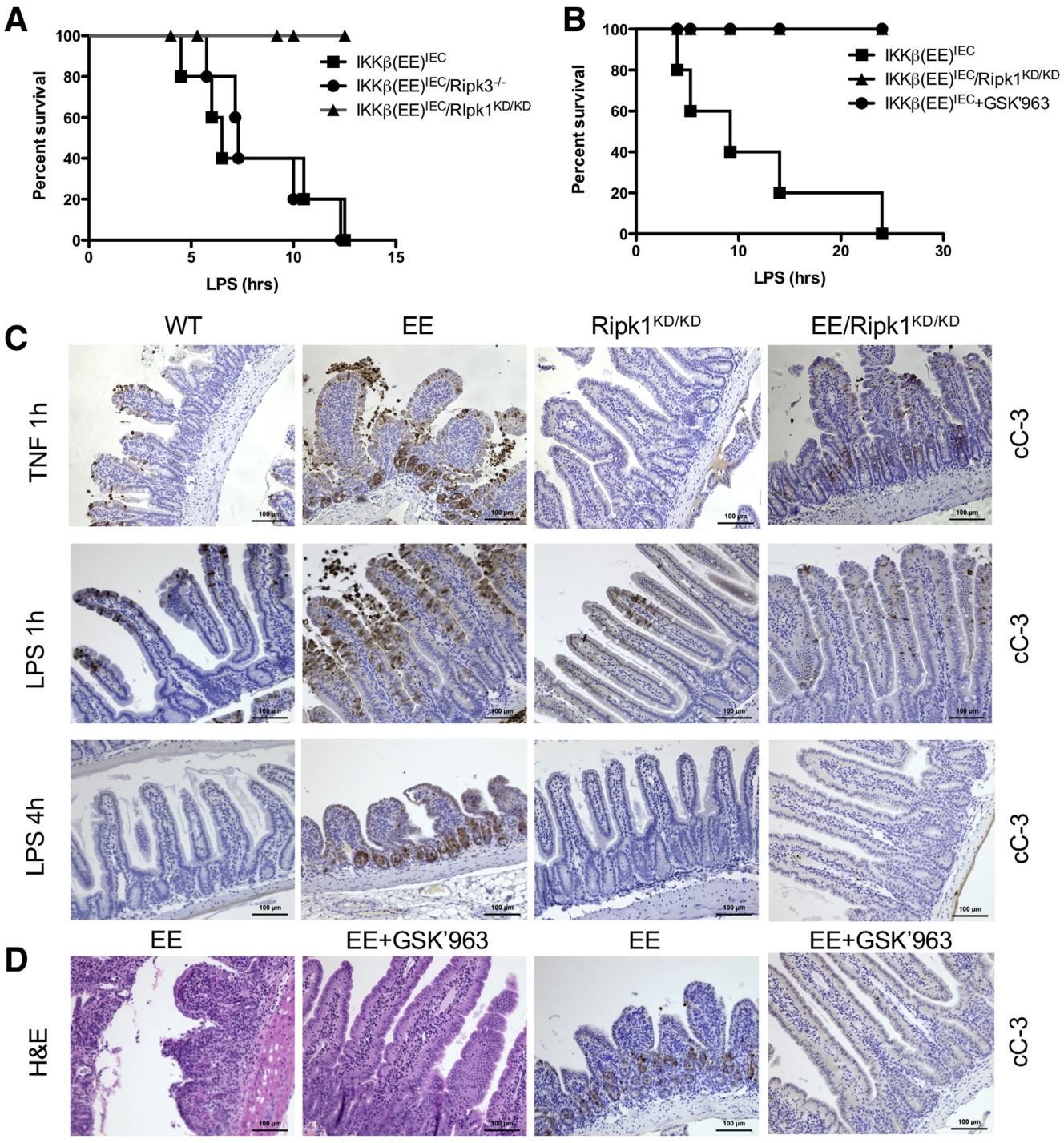

Figure 8. RIPK1 kinase activity is required for TNF-induced death in intestinal crypts. (*A*) *Ikkβ(EE)*^{IEC}, *Ikkβ(EE)*^{IEC}/*Ripk1*$^{D138N/D138N}$, and *Ikkβ(EE)*^{IEC}/*Ripk3*-/- mice were injected with LPS (0.5 mg/kg, *Escherichia coli O111:B4*) and their survival was monitored over a 36-hour period (n = 5 per group). (*B*) *Ikkβ(EE)*^{IEC} mice were injected with LPS in the absence or presence of GSK'963 (50 mg/kg) and their survival analyzed over a 36-hour period and compared with that of LPS-injected *Ikkβ(EE)*^{IEC}/*Ripk1*$^{D138N/D138N}$ mice (n = 5 per group). (*C*) The strains listed above along with WT mice were injected with TNF (2 μg intravenously) or LPS (0.5 mg/kg i.p.). Jejunal sections were collected at indicated times and stained for cC-3. Magnification bars: 100 μm. (*D*) *Ikkβ(EE)*^{IEC} were injected with LPS (0.5 mg/kg i.p) in the absence or presence of GSK'963 (50 mg/kg). Jejunal sections were collected after 4 hours of LPS injection and stained for H&E or cC-3. Magnification bars: 100 μm.

mL. CHX (25 μg/mL), zVAD-FMK (50 μM), BHA (10 μM), Nec-1 (100 μM), and DPI (5 μM) were purchased from Sigma. RIPK1 (Nec-1s: 50 nM and 963: 50 nM) and RIPK3 (843: 5 μM, 872: 5 μM) inhibitors were synthesized at GSK and purified before use at the previously determined doses.[30,31] For *in vivo* studies, BHA (20 mg/kg) and the

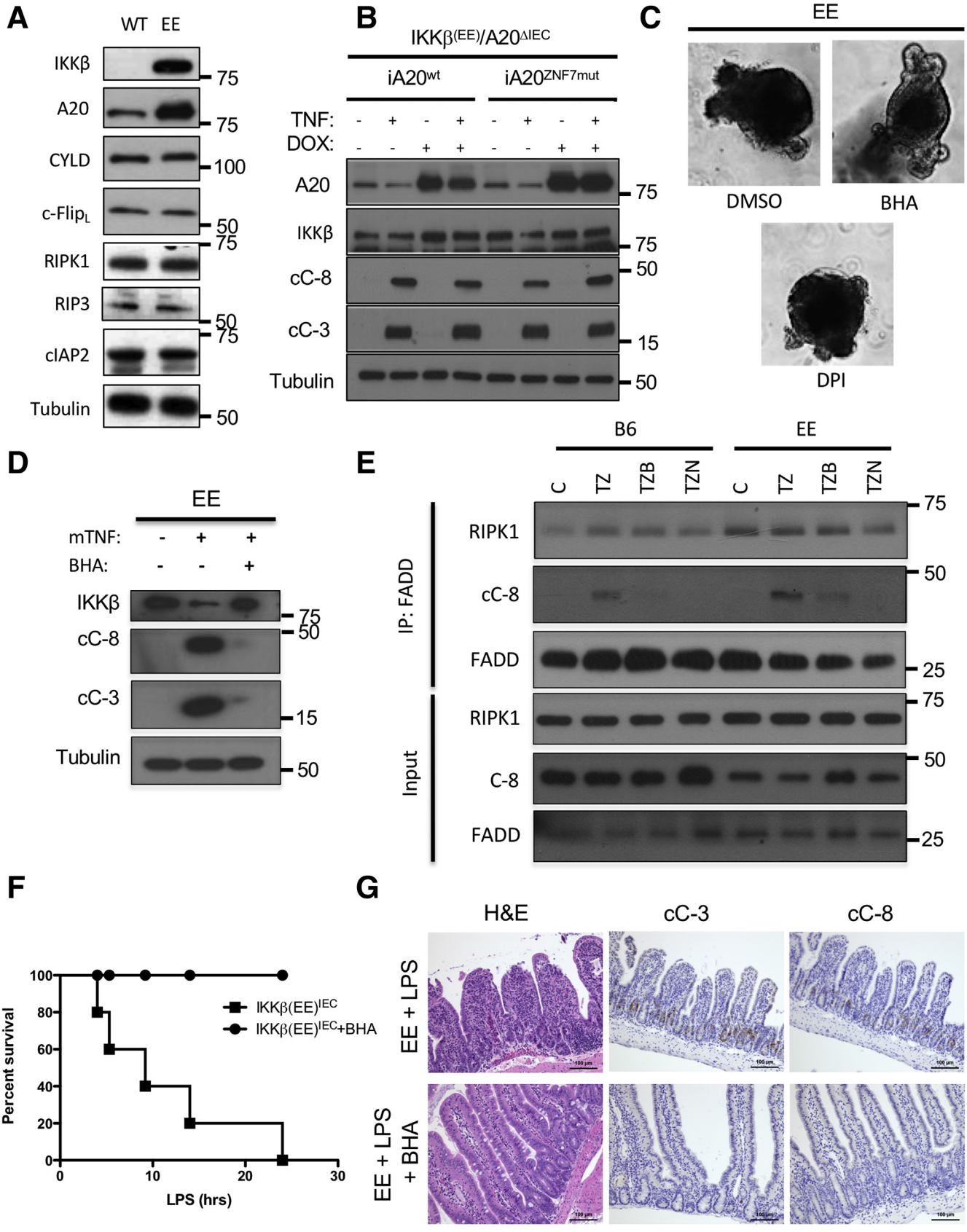
A
WT EE
IKKβ
A20
CYLD
c-Flip$_L$
RIPK1
RIP3
cIAP2
Tubulin
75
75
100
50
75
50
75
50
B
IKKβ$^{(EE)}$/A20^{ΔIEC}
iA20^{wt}
iA20^{ZNF7mut}
TNF: - + - + - + - +
DOX: - - + + - - + +
A20
IKKβ
cC-8
cC-3
Tubulin
75
75
50
15
50
C
EE
DMSO
BHA
DPI
D
EE
mTNF: - + +
BHA: - - +
IKKβ
cC-8
cC-3
Tubulin
75
50
15
50
E
B6
EE
C TZ TZB TZN C TZ TZB TZN
IP: FADD
RIPK1
cC-8
FADD
Input
RIPK1
C-8
FADD
75
50
25
75
50
25
F
Percent survival
100
80
60
40
20
0
0 10 20 30
LPS (hrs)
IKKβ(EE)^{IEC}
IKKβ(EE)^{IEC}+BHA
G
H&E
cC-3
cC-8
EE + LPS
EE + LPS + BHA

RIPK1 inhibitor GSK'963 (50 mg/kg) were dissolved in saline with 5% dimethyl sulfoxide and 6% Cavitron and were i.p. injected.

Human Samples

Archived specimens of ileum and colon for IHC analyses were obtained from patients who had undergone routine colonoscopy for clinical indications. Prospective ileum and colon specimens used for RNA analysis were obtained from patients with CD or UC and healthy control subjects undergoing colonoscopy as part of routine medical care at UCSD. The recruited participants had a diagnosis of CD or UC and were older than 18 years. Healthy control subjects were undergoing colonoscopy as part of routine colon cancer screening. Healthy control subjects were not included if they reported gastrointestinal symptoms. The clinical status of the patients was verified by chart review of all medical records, laboratory and pathologic data, and all specimens were deidentified before use. All participants provided written informed consent. The institutional review boards at UCSD and at VA San Diego Healthcare System approved the study.

RNAseq and Bioinformatics

Total RNA was isolated from human intestinal tissues and its quality was assessed on an Agilent Bioanalyzer (Santa Clara, CA). Samples that were determined to have an RNA Integrity Number of 7 or greater were used to generate RNA libraries using Illumina TruSeq Stranded Total RNA Sample Prep Kit starting with 100 ng of RNA. Libraries were then sequenced using the Illumina Hiseq2500 sequencer (San Diego, CA). *Ikkβ(EE)^{IEC}* expression array profiling was published[14] and submitted to GEO (GSE29701). The fastq files were aligned to human and mouse transcriptomes of the Genome Reference Consortium GRCh.37/hg19 and GRCm.38/mm10, respectively, using the STAR aligner.[54] Transcript-level counts were calculated with an expectation maximization algorithm RSEM.[55] Transcript-level summaries were processed into gene-level summaries by combining all transcript counts from the same gene. Gene counts from different samples were normalized and analyzed for differential expression using DESeq.[56] Because at least 1 of the samples does not have biologic replicates, we used an ansatz in which dispersion of gene counts is estimated from all available samples as if they were replicates. All presented measures of statistical significance should be viewed in this light. Where comparisons are made between expression patterns of human and the mouse model, we used the Homologene database to translate mouse genes into their human homologues, if such a homologue exists, and compared mouse expression data with their human counterparts.

Real-Time Quantitative Polymerase Chain Reaction

Intestinal human tissue from healthy control subjects and patients with CD was collected by colonoscopy and total RNA was extracted with Trizol (Invitrogen, Carlsbad, CA) and reverse-transcribed with random hexamers and Superscript II Kit (Invitrogen). Quantitative polymerase chain reaction (qPCR) was performed with SYBR Green PCR Master Mix Kit (Applied Biosystems, Foster City, CA). The relative amounts of each transcript were compared with those of GAPDH and normalized to untreated samples by the $^{\Delta\Delta}$Ct method. Primers are available on request.

Histologic Analysis and IHC

Intestines were removed, opened longitudinally, cleaned, processed as "Swiss rolls," and fixed in 10% phosphate-buffered formalin for 24 hours. Fixed tissues were embedded in paraffin, and 5 μm sections were prepared and stained with H&E. For IHC, sections from murine and human samples were incubated overnight at 4°C with anti-p65/RelA, anti-cC-3, or anti-cC-8 antibodies (1697, 9661, and 8592, respectively; Cell Signaling, Danvers, MA) at a 1:200 dilution. Antigen retrieval was with citrate buffer pH 6.0 at 96°C for 20 minutes. All sections were counterstained with hematoxylin and photographed using an Axioplan 200 microscope with AxioVision Release 4.5 software (Zeiss, Oberkochen, Germany).

Enteroid Isolation and Culture

Small intestinal organoids (enteroids) were cultured as described.[24] Briefly, crypts were collected from small intestines of mice after 30-minute incubation in phosphate-buffered saline (PBS; pH 7.4) containing 2-mM EDTA in 6°C. Enteroids were plated in Matrigel (BD Bioscience, San Jose, CA) and maintained in DMEM/F12 (Life Technologies, Carlsbad, CA) containing B27 and N2 supplements (Life Technologies), 1.25 mM N-acetyl L-cysteine (Sigma), 100 ng/mL noggin (GoldBio, St. Louis,

Figure 9. (***See previous page***). **TNF-induced apoptosis of IKKβ(EE)-expressing IEC involves ripoptosome formation and can be inhibited by BHA.** (*A*) WT and *Ikkβ(EE)^{IEC}* enteroids were IB analyzed with antibodies to the indicated proteins. (*B*) *Ikkβ(EE)^{IEC}*/A20$^{\Delta IEC}$ enteroids infected with the indicated A20 constructs and preincubated with doxycycline were stimulated without or with TNF (40 μg/mL) for 4 hours and IB analyzed with the indicated antibodies. (*C*) *Ikkβ(EE)^{IEC}* enteroids were incubated with dimethyl sulfoxide, BHA (10 μM), or diphenylene iodonium (5 μM) together with TNF (40 ng/mL) and photographed under brightfield 4 hours later. Original magnification ×200. (*D*) Lysates of *Ikkβ(EE)^{IEC}* enteroids treated with BHA and/or TNF as indicated were IB analyzed after 4 hours. (*E*) WT and *Ikkβ(EE)^{IEC}* enteroids were stimulated without (*C*) or with TNF together with zVAD (10 μg/mL) (TZ), BHA (TZB), or Nec-1 (50 nM) (TZN) for 2 hours. Complex IIb was isolated by FADD immunoprecipitation and IB analyzed with the indicated antibodies. (*F*) *Ikkβ(EE)^{IEC}* mice were treated with or without BHA (20 mg/kg), challenged with LPS (0.5 mg/kg *Escherichia coli O111:B4*), and their survival was monitored over a 36-hour period (n = 5 mice per group). (*G*) *Ikkβ(EE)^{IEC}* mice treated as above were analyzed 4 hours after LPS injection. Jejunal sections were stained with either H&E or antibodies to cC-8 or cC-3. Magnification bars: 100 μm. DMSO, dimethyl sulfoxide; DPI, diphenylene iodonium

MO), 50 ng/mL mEGF (Biosource, San Diego, CA), and 10% Rspo1-Fc-conditioned medium (the Rspo1-Fc-expressing cell line was a generous gift from Dr. Calvin Kuo, Stanford).

Immunoblotting and Immunoprecipitation

Whole cell extracts were obtained by lysing enteroids in ice-cold RIPA lysis buffer (Cell Signaling) containing 20 mM Tris-HCl, pH 7.5, 150 mM NaCl, 10 mM EDTA, 1% Triton X-100, and 1% deoxycholate, supplemented with a protease inhibitor cocktail (Roche, Basel, Switzerland). Proteins were separated by sodium dodecyl sulfate–polyacrylamide gel electrophoresis and transferred to nitrocellulose membranes that were incubated with antibodies against IKKβ (Millipore, Billerica, MA), A20 (Thermofisher, Waltham, MA), IκBα, p65, (Santa Cruz Biotechnology Inc, Santa Cruz, CA), RIPK1, IKKγ, and TNF (R&D Systems, Minneapolis, MN), RIPK3 (eBioscience, Waltham, MA), cC-3, cC-8, A20, and ERK1/2 (Cell Signaling), actin, and tubulin (Sigma). For immunoprecipitation, whole cell extracts were incubated with the indicated antibodies and Protein G Dynabeads (Life Technologies) overnight at 4°C. Immunocomplexes were washed with lysis buffer and analyzed by IB. To isolate protein complexes by coimmunoprecipitation, the indicated antibodies and cell lysates were incubated in 10 mM Tris, pH 7.4, 150 mM NaCl, and 0.2% Nonident P-40.

Proliferation Assay

Enteroids in Matrigel were stimulated with interleukin-22 (10 ng/mL) for 24 hours. EdU (Click-iT EdU Alexa Fluor 594 Imaging Kit, Thermo Fisher C10339) was added at 10 μM 2 hours before fixation. EdU staining was performed as indicated by the manufacturer.

Cell Survival Assay

3-.4,5-dimethylthiazole-2-yl]-2,5-diphenyltetrazolium bromide (MTT) was dissolved in PBS at 5 mg/mL. Organoids were stimulated as indicated and 4 hours post-treatment MTT was added to the media to a final concentration of 0.5 mg/mL. Thirty minutes post-MTT, cell viability was assessed through microscopic visualization of organoids and quantified.

Immunofluorescence

Enteroids in Matrigel were fixed with 4% paraformaldehyde overnight at 4°C. Fixed enteroids were blocked with PBS containing 0.2% Triton X-100 and 1% bovine serum albumin for 30 minutes, immunostained with primary antibodies overnight at 4°C and with Alexa Fluor 594-conjugated goat antirabbit IgG secondary antibody for 1 hour at room temperature. Immunostained enteroids were gently mounted on the slide glass and imaged under the Zeiss confocal microscope.

Constructs and Lentivirus Transduction of Enteroids

The inducible-IKKβ(EE) lentiviral expression constructs were made by subcloning PCR amplified *att*B-flanked IKKβ(EE),[57] or A20[58] and the different A20 mutants[59] cDNAs were PCR amplified and cloned into pINDUCER20[60] using the Gateway Clonase II system (Life Technologies). All constructs were verified by sequencing.

The lentiviral constructs were transfected along with pMD2.G (Addgene, Plasmid 12259) and psPAX2 (Addgene, Plasmid 12260) into 293T cells to produce viral particles used to infect enteroids as described.[61] Briefly, 2 days before virus infection, enteroids were supplemented with 50% Wnt3a conditioned medium (the Wnt3a-expressing cell line was a generous gift from Dr. Karl Willert, UCSD) and 10 mM nicotinamide. Single cells were obtained by digesting the enteroids with TrypLE (Life Technologies) for 5 minutes at 37°C. Cells were mixed with high-titer lentivirus plus polybrene (8 μg/mL, Santa Cruz) and Y-27632 (10 μM, Sigma) in a 48-well culture plate and centrifuged at 600 × *g* at 32°C for 60 minutes, followed by 5 hours incubation at 37°C. Cells were then plated in Matrigel and cultured in media with 50% Wnt3a, nicotinamide, and Y-27632 for 2 days, followed by selection with puromycin (1 μg/mL) or G418 (800 ng/mL) in regular media for 1 week.

Statistical Analysis

Data are expressed as means ± standard error. For comparison between 2 groups, a 2-tailed Student *t* test or a Mann-Whitney test was applied depending on the normality of the distribution of the variables. All statistical analyses were performed using GraphPad Prism statistical package. Results were considered significant at $P < .05$.

References

1. Abraham C, Cho JH. Inflammatory bowel disease. N Engl J Med 2009;361:2066–2078.
2. Gunther C, Neumann H, Neurath MF, Becker C. Apoptosis, necrosis and necroptosis: cell death regulation in the intestinal epithelium. Gut 2013;62:1062–1071.
3. Khor B, Gardet A, Xavier RJ. Genetics and pathogenesis of inflammatory bowel disease. Nature 2011; 474:307–317.
4. Okamoto R, Watanabe M. Role of epithelial cells in the pathogenesis and treatment of inflammatory bowel disease. J Gastroenterol 2016;51:11–21.
5. Neurath MF, Travis SP. Mucosal healing in inflammatory bowel diseases: a systematic review. Gut 2012; 61:1619–1635.
6. Vereecke L, Beyaert R, van Loo G. The ubiquitin-editing enzyme A20 (TNFAIP3) is a central regulator of immunopathology. Trends Immunol 2009;30:383–391.
7. Kaser A, Zeissig S, Blumberg RS. Inflammatory bowel disease. Ann Rev Immunol 2010;28:573–621.

8. Zeissig S, Bojarski C, Buergel N, Mankertz J, Zeitz M, Fromm M, Schulzke JD. Downregulation of epithelial apoptosis and barrier repair in active Crohn's disease by tumour necrosis factor alpha antibody treatment. Gut 2004;53:1295–1302.
9. Lin A, Karin M. NF-kappaB in cancer: a marked target. Semin Cancer Biol 2003;13:107–114.
10. Egan LJ, Eckmann L, Greten FR, Chae S, Li ZW, Myhre GM, Robine S, Karin M, Kagnoff MF. IkappaB-kinasebeta-dependent NF-kappaB activation provides radioprotection to the intestinal epithelium. Proc Natl Acad Sci U S A 2004;101:2452–2457.
11. Chen LW, Egan L, Li ZW, Greten FR, Kagnoff MF, Karin M. The two faces of IKK and NF-kappaB inhibition: prevention of systemic inflammation but increased local injury following intestinal ischemia-reperfusion. Nat Med 2003;9:575–581.
12. Nenci A, Becker C, Wullaert A, Gareus R, van Loo G, Danese S, Huth M, Nikolaev A, Neufert C, Madison B, Gumucio D, Neurath MF, Pasparakis M. Epithelial NEMO links innate immunity to chronic intestinal inflammation. Nature 2007;446:557–561.
13. Garcia-Carbonell R, Wong J, Kim JY, Close LA, Boland BS, Wong TL, Harris PA, Ho SB, Das S, Ernst PB, Sasik R, Sandborn WJ, Bertin J, Gough PJ, Chang JT, Kelliher M, Boone D, Guma M, Karin M. Elevated A20 promotes TNF-induced and RIPK1-dependent intestinal epithelial cell death. Proc Natl Acad Sci U S A 2018; 115:E9192–E9200.
14. Guma M, Stepniak D, Shaked H, Spehlmann ME, Shenouda S, Cheroutre H, Vicente-Suarez I, Eckmann L, Kagnoff MF, Karin M. Constitutive intestinal NF-kappaB does not trigger destructive inflammation unless accompanied by MAPK activation. J Exp Med 2011; 208:1889–1900.
15. Pasparakis M, Vandenabeele P. Necroptosis and its role in inflammation. Nature 2015;517:311–320.
16. Weinlich R, Green DR. The two faces of receptor interacting protein kinase-1. Mol Cell 2014;56:469–480.
17. Wang L, Du F, Wang X. TNF-alpha induces two distinct caspase-8 activation pathways. Cell 2008;133:693–703.
18. Kanayama A, Seth RB, Sun L, Ea CK, Hong M, Shaito A, Chiu YH, Deng L, Chen ZJ. TAB2 and TAB3 activate the NF-kappaB pathway through binding to polyubiquitin chains. Mol Cell 2004;15:535–548.
19. Micheau O, Thome M, Schneider P, Holler N, Tschopp J, Nicholson DW, Briand C, Grutter MG. The long form of FLIP is an activator of caspase-8 at the Fas death-inducing signaling complex. J Biol Chem 2002; 277:45162–45171.
20. Feng P, Liang C, Shin YC, Xiaofei E, Zhang W, Gravel R, Wu TT, Sun R, Usherwood E, Jung JU. A novel inhibitory mechanism of mitochondrion-dependent apoptosis by a herpesviral protein. PLoS Pathog 2007;3:e174.
21. O'Donnell MA, Perez-Jimenez E, Oberst A, Ng A, Massoumi R, Xavier R, Green DR, Ting AT. Caspase 8 inhibits programmed necrosis by processing CYLD. Nat Cell Biol 2011;13:1437–1442.
22. Rogler G, Brand K, Vogl D, Page S, Hofmeister R, Andus T, Knuechel R, Baeuerle PA, Scholmerich J, Gross V. Nuclear factor kappaB is activated in macrophages and epithelial cells of inflamed intestinal mucosa. Gastroenterology 1998;115:357–369.
23. Leal RF, Planell N, Kajekar R, Lozano JJ, Ordas I, Dotti I, Esteller M, Masamunt MC, Parmar H, Ricart E, Panes J, Salas A. Identification of inflammatory mediators in patients with Crohn's disease unresponsive to anti-TNFalpha therapy. Gut 2015;64:233–242.
24. Sato T, Vries RG, Snippert HJ, van de Wetering M, Barker N, Stange DE, van Es JH, Abo A, Kujala P, Peters PJ, Clevers H. Single Lgr5 stem cells build crypt-villus structures in vitro without a mesenchymal niche. Nature 2009;459:262–265.
25. Kreuz S, Siegmund D, Scheurich P, Wajant H. NF-kappaB inducers upregulate cFLIP, a cycloheximide-sensitive inhibitor of death receptor signaling. Mol Cell Biol 2001;21:3964–3973.
26. Kawakami H, Tomita M, Matsuda T, Ohta T, Tanaka Y, Fujii M, Hatano M, Tokuhisa T, Mori N. Transcriptional activation of survivin through the NF-kappaB pathway by human T-cell leukemia virus type I tax. Int J Cancer 2005; 115:967–974.
27. Ofengeim D, Yuan J. Regulation of RIP1 kinase signalling at the crossroads of inflammation and cell death. Nat Rev Cell Biol 2013;14:727–736.
28. Degterev A, Hitomi J, Germscheid M, Ch'en IL, Korkina O, Teng X, Abbott D, Cuny GD, Yuan C, Wagner G, Hedrick SM, Gerber SA, Lugovskoy A, Yuan J. Identification of RIP1 kinase as a specific cellular target of necrostatins. Nat Chem Biol 2008; 4:313–321.
29. Takahashi N, Duprez L, Grootjans S, Cauwels A, Nerinckx W, DuHadaway JB, Goossens V, Roelandt R, Van Hauwermeiren F, Libert C, Declercq W, Callewaert N, Prendergast GC, Degterev A, Yuan J, Vandenabeele P. Necrostatin-1 analogues: critical issues on the specificity, activity and in vivo use in experimental disease models. Cell Death Dis 2012;3:e437.
30. Mandal P, Berger SB, Pillay S, Moriwaki K, Huang C, Guo H, Lich JD, Finger J, Kasparcova V, Votta B, Ouellette M, King BW, Wisnoski D, Lakdawala AS, DeMartino MP, Casillas LN, Haile PA, Sehon CA, Marquis RW, Upton J, Daley-Bauer LP, Roback L, Ramia N, Dovey CM, Carette JE, Chan FK, Bertin J, Gough PJ, Mocarski ES, Kaiser WJ. RIP3 induces apoptosis independent of pronecrotic kinase activity. Mol Cell 2014;56:481–495.
31. Berger SB, Harris P, Nagilla R, Kasparcova V, Hoffman S, Swift B, Dare L, Schaeffer M, Capriotti C, Ouellette M, King BW, Wisnoski D, Reilly M, Marquis RW, Bertin J, Gough PJ. Characterization of GSK'963: a structurally distinct, potent and selective inhibitor of RIP1 kinase. Cell Death Discov 2015;1:15009.
32. Polykratis A, Hermance N, Zelic M, Roderick J, Kim C, Van TM, Lee TH, Chan FK, Pasparakis M, Kelliher MA. Cutting edge: RIPK1 Kinase inactive mice are viable and protected from TNF-induced necroptosis in vivo. J Immunol 2014;193:1539–1543.
33. Newton K, Sun X, Dixit VM. Kinase RIP3 is dispensable for normal NF-kappa Bs, signaling by the B-cell and T-

cell receptors, tumor necrosis factor receptor 1, and Toll-like receptors 2 and 4. Mol Cell Biol 2004; 24:1464–1469.
34. Zhang DW, Shao J, Lin J, Zhang N, Lu BJ, Lin SC, Dong MQ, Han J. RIP3, an energy metabolism regulator that switches TNF-induced cell death from apoptosis to necrosis. Science 2009;325:332–336.
35. Vandenabeele P, Declercq W, Van Herreweghe F, Vanden Berghe T. The role of the kinases RIP1 and RIP3 in TNF-induced necrosis. Sci Signal 2010;3:re4.
36. Vanden Berghe T, Linkermann A, Jouan-Lanhouet S, Walczak H, Vandenabeele P. Regulated necrosis: the expanding network of non-apoptotic cell death pathways. Nat Rev Mol Cell Biol 2014;15:135–147.
37. Kim YS, Morgan MJ, Choksi S, Liu ZG. TNF-induced activation of the Nox1 NADPH oxidase and its role in the induction of necrotic cell death. Mol Cell 2007; 26:675–687.
38. Shindo R, Kakehashi H, Okumura K, Kumagai Y, Nakano H. Critical contribution of oxidative stress to TNFalpha-induced necroptosis downstream of RIPK1 activation. Biochem Biophys Res Commun 2013; 436:212–216.
39. Zhang Y, Su SS, Zhao S, Yang Z, Zhong CQ, Chen X, Cai Q, Yang ZH, Huang D, Wu R, Han J. RIP1 autophosphorylation is promoted by mitochondrial ROS and is essential for RIP3 recruitment into necrosome. Nat Commun 2017;8:14329.
40. Matsuzawa-Ishimoto Y, Shono Y, Gomez LE, Hubbard-Lucey VM, Cammer M, Neil J, Dewan MZ, Lieberman SR, Lazrak A, Marinis JM, Beal A, Harris PA, Bertin J, Liu C, Ding Y, van den Brink MRM, Cadwell K. Autophagy protein ATG16L1 prevents necroptosis in the intestinal epithelium. J Exp Med 2017;214:3687–3705.
41. Pott J, Kabat AM, Maloy KJ. Intestinal epithelial cell autophagy is required to protect against TNF-induced apoptosis during chronic colitis in mice. Cell Host Microbe 2018;23:191–202.
42. Aden K, Tran F, Ito G, Sheibani-Tezerji R, Lipinski S, Kuiper JW, Tschurtschenthaler M, Saveljeva S, Bhattacharyya J, Hasler R, Bartsch K, Luzius A, Jentzsch M, Falk-Paulsen M, Stengel ST, Welz L, Schwarzer R, Rabe B, Barchet W, Krautwald S, Hartmann G, Pasparakis M, Blumberg RS, Schreiber S, Kaser A, Rosenstiel P. ATG16L1 orchestrates interleukin-22 signaling in the intestinal epithelium via cGAS-STING. J Exp Med 2018;215:2868–2886.
43. Anderson CA, Boucher G, Lees CW, Franke A, D'Amato M, Taylor KD, Lee JC, Goyette P, Imielinski M, Latiano A, Lagace C, Scott R, Amininejad L, Bumpstead S, Baidoo L, Baldassano RN, Barclay M, Bayless TM, Brand S, Buning C, Colombel JF, Denson LA, De Vos M, Dubinsky M, Edwards C, Ellinghaus D, Fehrmann RS, Floyd JA, Florin T, Franchimont D, Franke L, Georges M, Glas J, Glazer NL, Guttery SL, Hamiltonians T, Hayward NK, Hugo JP, Jobin G, Lukens D, Lawrence I, Lemann M, Levine A, Lobule C, Louis E, McGovern DP, Milla M, Montgomery GW, Morley KI, Mowat C, Ng A, Newman W, Popoff RA, Papa L, Palmieri O, Peyrin-Biroulet L, Panes J, Phillips A, Prescott NJ, Proctor DD, Roberts R, Russell R, Rutgeerts P, Sanderson J, Sans M, Schumm P, Seibold F, Sharma Y, Simms LA, Seielstad M, Steinhart AH, Targan SR, van den Berg LH, Vatn M, Verspaget H, Walters T, Wijmenga C, Wilson DC, Westra HJ, Xavier RJ, Zhao ZZ, Ponsioen CY, Andersen V, Torkvist L, Gazouli M, Anagnou NP, Karlsen TH, Kupcinskas L, Sventoraityte J, Mansfield JC, Kugathasan S, Silverberg MS, Halfvarson J, Rotter JI, Mathew CG, Griffiths AM, Gearry R, Ahmad T, Brant SR, Chamaillard M, Satsangi J, Cho JH, Schreiber S, Daly MJ, Barrett JC, Parkes M, Annese V, Hakonarson H, Radford-Smith G, Duerr RH, Vermeire S, Weersma RK, Rioux JD. Meta-analysis identifies 29 additional ulcerative colitis risk loci, increasing the number of confirmed associations to 47. Nat Genet 2011;43:246–252.
44. Franke A, McGovern DP, Barrett JC, Wang K, Radford-Smith GL, Ahmad T, Lees CW, Balschun T, Lee J, Roberts R, Anderson CA, Bis JC, Bumpstead S, Ellinghaus D, Festen EM, Georges M, Green T, Haritunians T, Jostins L, Latiano A, Mathew CG, Montgomery GW, Prescott NJ, Raychaudhuri S, Rotter JI, Schumm P, Sharma Y, Simms LA, Taylor KD, Whiteman D, Wijmenga C, Baldassano RN, Barclay M, Bayless TM, Brand S, Buning C, Cohen A, Colombel JF, Cottone M, Stronati L, Denson T, De Vos M, D'Inca R, Dubinsky M, Edwards C, Florin T, Franchimont D, Gearry R, Glas J, Van Gossum A, Guthery SL, Halfvarson J, Verspaget HW, Hugot JP, Karban A, Laukens D, Lawrance I, Lemann M, Levine A, Libioulle C, Louis E, Mowat C, Newman W, Panes J, Phillips A, Proctor DD, Regueiro M, Russell R, Rutgeerts P, Sanderson J, Sans M, Seibold F, Steinhart AH, Stokkers PC, Torkvist L, Kullak-Ublick G, Wilson D, Walters T, Targan SR, Brant SR, Rioux JD, D'Amato M, Weersma RK, Kugathasan S, Griffiths AM, Mansfield JC, Vermeire S, Duerr RH, Silverberg MS, Satsangi J, Schreiber S, Cho JH, Annese V, Hakonarson H, Daly MJ, Parkes M. Genome-wide meta-analysis increases to 71 the number of confirmed Crohn's disease susceptibility loci. Nat Genet 2010;42:1118–1125.
45. Liu JZ, van Sommeren S, Huang H, Ng SC, Alberts R, Takahashi A, Ripke S, Lee JC, Jostins L, Shah T, Abedian S, Cheon JH, Cho J, Dayani NE, Franke L, Fuyuno Y, Hart A, Juyal RC, Juyal G, Kim WH, Morris AP, Poustchi H, Newman WG, Midha V, Orchard TR, Vahedi H, Sood A, Sung JY, Malekzadeh R, Westra HJ, Yamazaki K, Yang SK, International Multiple Sclerosis Genetics C; , International IBDGC, Barrett JC, Alizadeh BZ, Parkes M, Bk T, Daly MJ, Kubo M, Anderson CA, Weersma RK. Association analyses identify 38 susceptibility loci for inflammatory bowel disease and highlight shared genetic risk across populations. Nat Genet 2015;47:979–986.
46. Greten FR, Eckmann L, Greten TF, Park JM, Li ZW, Egan LJ, Kagnoff MF, Karin M. IKKbeta links inflammation and tumorigenesis in a mouse model of colitis-associated cancer. Cell 2004;118:285–296.
47. Pereira C, Gracio D, Teixeira JP, Magro F. Oxidative stress and DNA damage: implications in inflammatory bowel disease. Inflamm Bowel Dis 2015; 21:2403–2417.

48. Shaked H, Hofseth LJ, Chumanevich A, Chumanevich AA, Wang J, Wang Y, Taniguchi K, Guma M, Shenouda S, Clevers H, Harris CC, Karin M. Chronic epithelial NF-kappaB activation accelerates APC loss and intestinal tumor initiation through iNOS up-regulation. Proc Natl Acad Sci U S A 2012;109:14007–14012.
49. Lakatos PL, Lakatos L. Risk for colorectal cancer in ulcerative colitis: changes, causes and management strategies. World J Gastroenterol 2008;14:3937–3947.
50. Abraham BP. Cancer surveillance in ulcerative colitis and Crohn's disease: new strategies. Curr Opin Gastroenterol 2016;32:32–37.
51. Brain O, Allan P, Simmons A. NOD2-mediated autophagy and Crohn disease. Autophagy 2010;6:412–414.
52. Newton K, Dugger DL, Wickliffe KE, Kapoor N, de Almagro MC, Vucic D, Komuves L, Ferrando RE, French DM, Webster J, Roose-Girma M, Warming S, Dixit VM. Activity of protein kinase RIPK3 determines whether cells die by necroptosis or apoptosis. Science 2014;343:1357–1360.
53. Rott HD, Fahsold R. Tuberous sclerosis in two sibs of normal parents. Clin Genet 1991;39:306–308.
54. Dobin A, Davis CA, Schlesinger F, Drenkow J, Zaleski C, Jha S, Batut P, Chaisson M, Gingeras TR. STAR: ultrafast universal RNA-seq aligner. Bioinformatics 2013;29:15–21.
55. Li B, Dewey CN. RSEM: accurate transcript quantification from RNA-Seq data with or without a reference genome. BMC Bioinformatics 2011;12:323.
56. Anders S, Huber W. Differential expression analysis for sequence count data. Genome Biol 2010;11:R106.
57. Delhase M, Hayakawa M, Chen Y, Karin M. Positive and negative regulation of IkappaB kinase activity through IKKbeta subunit phosphorylation. Science 1999;284:309–313.
58. Wertz IE, O'Rourke KM, Zhou H, Eby M, Aravind L, Seshagiri S, Wu P, Wiesmann C, Baker R, Boone DL, Ma A, Koonin EV, Dixit VM. De-ubiquitination and ubiquitin ligase domains of A20 downregulate NF-kappaB signalling. Nature 2004;430:694–699.
59. Lu TT, Onizawa M, Hammer GE, Turer EE, Yin Q, Damko E, Agelidis A, Shifrin N, Advincula R, Barrera J, Malynn BA, Wu H, Ma A. Dimerization and ubiquitin mediated recruitment of A20, a complex deubiquitinating enzyme. Immunity 2013;38:896–905.
60. Meerbrey KL, Hu G, Kessler JD, Roarty K, Li MZ, Fang JE, Herschkowitz JI, Burrows AE, Ciccia A, Sun T, Schmitt EM, Bernardi RJ, Fu X, Bland CS, Cooper TA, Schiff R, Rosen JM, Westbrook TF, Elledge SJ. The pINDUCER lentiviral toolkit for inducible RNA interference in vitro and in vivo. Proc Natl Acad Sci U S A 2011;108:3665–3670.
61. Koo BK, Stange DE, Sato T, Karthaus W, Farin HF, Huch M, van Es JH, Clevers H. Controlled gene expression in primary Lgr5 organoid cultures. Nat Methods 2012;9:81–83.

Received June 7, 2019. Accepted October 3, 2019.

Correspondence
Address correspondence to: Monica Guma, MD, PhD, Department of Rheumatology, University of California San Diego, San Diego Digestive Disease Research Center, 9500 Gilman Drive, San Diego, California 92093. e-mail: mguma@ucsd.edu; fax: (858) 534-8158; and Michael Karin, Department of Pharmacology, University of California San Diego, San Diego, CA 92093. e-mail: karinoffice@ucsd.edu.

Acknowledgements
The authors acknowledge Genentech and Dr. Vishva Dixit for the provision of *Rip3*$^{-/-}$ mice. All authors had access to the study data and had reviewed and approved the final manuscript.

Author contributions
Jerry Wong, Monica Guma, and Michael Karin designed the study. Jerry Wong, Monica Guma, Ricard Garcia-Carbonell, Matija Zelic, Shih-Jing Yao, and Shalin A. Desai performed research. Philip A. Harris, Brigid S Boland, Joan Font-Burgada, Koji Taniguchi, Soumita Das, Núria Planell, Azucena Salas, John Bertin, Manolis Pasparakis, Pete J. Gough, and Michelle Kelliher contributed new constructs, chemical inhibitors, enteroid isolation, mice and human inflammatory bowel disease samples, and transcriptome data. Jerry Wong, Monica Guma, Ricard Garcia-Carbonell, and Michael Karin analyzed data. Jerry Wong, Ricard Garcia-Carbonell, Monica Guma, and Michael Karin wrote the paper.

Conflicts of interest
These authors disclose the following: Philip A. Harris, John Bertin, and Pete J. Gough are employees and shareholders of GlaxoSmithKline. The remaining authors disclose no conflicts.

Funding
Supported by fellowships from the Canadian Institutes of Health Research (J.W.) and Boehringer-Ingelheim Fonds (R.G.-C.); the National Institutes of Health 1K08AR064834 (M.G.), R01AI075118 (M. Kelliher), and T32DK007202 (B.S.B.); M.P. was funded by the ERC (2012-ADG_20120314), DFG (SFB670, SFB829, SPP1656), European Commission FP7 grants 223404 (Masterswitch) and 223151 (InflaCare), the Deutsche Krebshilfe (Grant 110302), and the Helmholtz Alliance Preclinical Comprehensive Cancer Center; M.K. was supported by NIH R01AI043477, is an American Cancer Society Research Professor, and holds the Ben and Wanda Hildyard Chair for Mitochondrial and Metabolic Diseases. M.G. and M. Karin were also supported by GlaxoSmithKline.